Lithos 212–215 (2015) 231–246

Contents lists available at ScienceDirect

Lithos

journal homepage: www.elsevier.com/locate/lithos

Geochronological and geochemical constraints on the origin of clastic meta-sedimentary rocks associated with the Yuanjiacun BIF from the Lüliang Complex, North China

Changle Wang [a,b], Lianchang Zhang [a,*], Yanpei Dai [a,b], Caiyun Lan [b,c]

[a] Key Laboratory of Mineral Resources, Institute of Geology and Geophysics, Chinese Academy of Sciences, Beijing 100029, China
[b] University of Chinese Academy of Sciences, Beijing 100049, China
[c] Guangzhou Institute of Geochemistry, Chinese Academy of Sciences, Guangdong, Guangzhou 510640, China

ARTICLE INFO

Article history:
Received 6 May 2014
Accepted 14 November 2014
Available online 27 November 2014

Keywords:
Yuanjiacun Formation
Lüliang Complex
Trans-North China Orogen
Detrital zircon
Geochemistry
Paleoproterozoic

ABSTRACT

The Lüliang Complex is situated in the central part of the western margin of the Trans-North China Orogen (TNCO) in the North China Craton (NCC), and consists of metamorphic volcanic and sedimentary rocks and granitoid intrusions. The Yuanjiacun Formation metasediments occupy roughly the lowest part of the Lüliang Group and are mainly represented by well-bedded meta-pelites (chlorite schists and sericite–chlorite phyllites), banded iron formations (BIFs) and meta-arenites (sericite schists), which have undergone greenschist-facies metamorphism. The youngest group of detrital zircons from the meta-arenite samples constrains their maximum depositional age at ~2350 Ma. In combination with previous geochronological studies on meta-volcanic rocks in the overlying Jinzhouyu Formation, the depositional age of the Yuanjiacun Formation can be constrained between 2350 and 2215 Ma. The metasediments have suffered varying degrees of source weathering, measured using widely employed weathering indices (e.g., CIA, CIW, PIA and Th/U ratios). Source rocks of the low-Al meta-pelites have undergone severe chemical weathering, whereas those of the meta-arenites and high-Al meta-pelites have suffered relatively moderate chemical weathering. Significant secondary K addition is recognized in the A–CN–K diagram for most of the studied samples. Diagnostic geochemical features like the Al_2O_3/TiO_2 values, trace element ratios (e.g., Th/Sc) and REE patterns, suggest that the meta-arenites and high-Al meta-pelites are predominantly derived from felsic igneous sources, whereas the low-Al meta-pelites are sourced mainly from mafic rocks. Coupled with Nd isotopic data, it is proposed that the meta-arenites and high-Al meta-pelites were sedimentary erosion products of the less differential felsic terrain (likely the old upper continental crust). The low-Al meta-pelites, however, have geochemical affinities with both pelite- and BIF-like components, suggesting that they were mixtures of these two sediments. Moreover, the U–Pb ages of detrital zircons from the Yuanjiacun metasediments yield three age populations of 2.8–2.65 Ga, 2.6–2.5 Ga and 2.5–2.35 Ga. The dominant Archean detrital zircons were most likely sourced from both the Archean igneous rocks in the Hengshan–Wutai–Fuping belt and old hidden Archean basement rocks in the Western Block, whereas the subordinate Paleoproterozoic detrital zircons were probably derived from the granitoid plutons within this age range in the Lüliang Complex. Taking the geochemical and geochronological data together, the Yuanjiacun Formation is interpreted as having been deposited in a passive margin setting (likely the eastern margin of the Western Block), most probably on a stable continental shelf.

1. Introduction

As one of the oldest orogenic belts containing high-pressure granulites and retrograded eclogites in the world, the Trans-North China Orogen (TNCO) has been interpreted as a Paleoproterozoic collisional orogen, along which the Eastern and Western Blocks were amalgamated to form the coherent basement of the North China Craton (NCC) at ~1.85 Ga (Guo et al., 2002, 2005; Liu et al., 2006; Zhao et al., 1998, 2005). Available geochronological and geochemical data show that the ~2.5 Ga geological events in the TNCO are related to the volcanic arc, producing granite–greenstone terranes like the Wutai and Dengfeng Complexes (Wilde and Zhao, 2005; Zhao et al., 2007). However, major controversy still surrounds the Paleoproterozoic tectonic evolution of the TNCO between 2500 and 1850 Ma.

The Lüliang Complex is situated in the central segment of the western margin of the TNCO and consists of Paleoproterozoic metamorphic volcanic and sedimentary rocks and granitoid intrusions (Fig. 1). Recent geochronological data reveal that the entire Lüliang Complex is considered to be composed exclusively of Paleoproterozoic rocks without any

* Corresponding author. Tel.: +86 10 82998185; fax: +86 10 62010846.
E-mail address: lczhang@mail.iggcas.ac.cn (L. Zhang).

http://dx.doi.org/10.1016/j.lithos.2014.11.015
0024-4937/

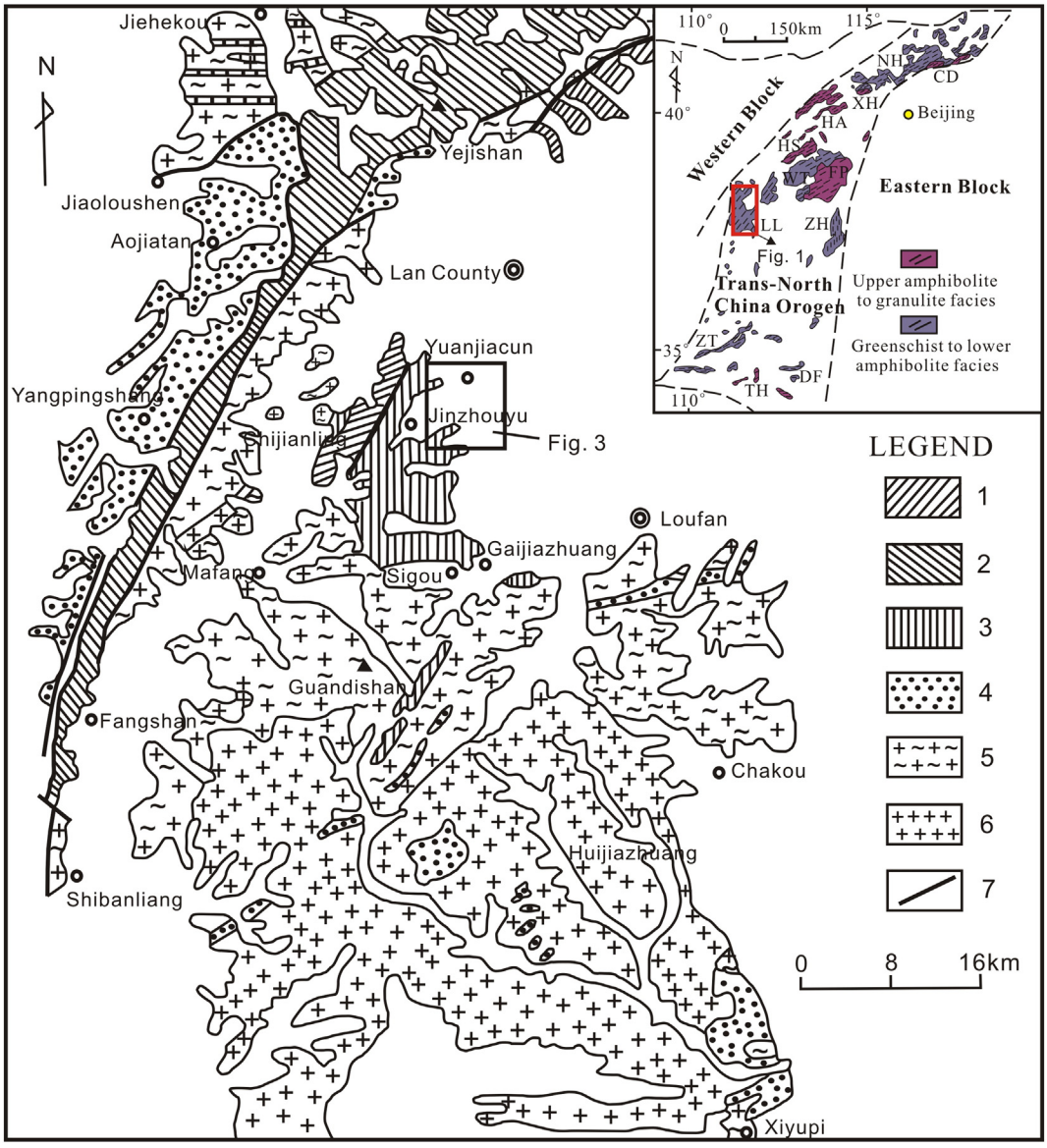

Fig. 1. Geological sketch of the Paleoproterozoic Lüling Complex (modified from Wan et al., 2000), showing geological distribution of the Lanhe Group (1), Yejishan Group (2), Lüliang Group (3), Jiehekou Group (4), gneissic granites (5), granites (6) and main faults (7) and the geological relationships among these units. The map insert shows the location of the Lüliang Complex in the North China Craton (revised after Zhao et al., 2005). Abbreviations for metamorphic complexes: CD, Chengde; DF, Dengfeng; FP, Fuping; HA, Huai'an; HS, Hengshan; LL, Lüliang; NH, Northern Hebei; TH, Taihua; WT, Wutai; XH, Xuanhua; ZH, Zanhuang; and ZT, Zhongtiao.

Archean components (Geng et al., 2000, 2004; Wan et al., 2000, 2006a; Yu et al., 1997a). The Lüliang Group, located in the central part of the Lüliang area, comprises greenschist- to amphibolite-facies metamorphosed sedimentary rocks with banded iron formations (BIFs) in the lower sequence and metamorphosed volcanic rocks in the upper part of the sequence. Based on the geochemistry of these 2.3–2.1 Ga meta-volcanic rocks, the Lüliang Group was considered to have formed in a rift environment (Geng et al., 2003; Yu et al., 1997b) or a magmatic arc system (Liu et al., 2012). Only the geochemical studies of these igneous rocks, however, cannot precisely constrain the tectonic setting of the underlying clastic meta-sediments and BIFs.

Geochemical and Nd isotopic data from clastic sedimentary rocks have been used to evaluate the nature of their provenance and weathering processes, as well as to identify the corresponding tectonic setting and understand crust–mantle evolution (Cullers, 1994a; McLennan et al., 1995; Taylor and McLennan, 1985). In this contribution, we first present an integrated study of major and trace element geochemical and Sm–Nd isotopic data, as well as zircon U–Pb ages of the meta-sedimentary rocks from the Yuanjiacun Formation in the lowest part of the Lüliang Group (see the Appendices for details). Combining with previous limited geochronological data from the overlying volcanic rocks, these data will not only provide constraints on their depositional age and provenance and tectonic setting but also gain an insight into the early Paleoproterozoic tectonic evolution of the TNCO.

2. Geological background

2.1. Geology of the Lüliang Complex

As mentioned above, the basement of the NCC can be divided into the Eastern and Western Blocks and the intervening TNCO (Zhao et al., 2005). The TNCO is a nearly south–north-trending zone that is 100–300 km wide and ~1200 km long (Fig. 1). Basement rocks of the orogen consist of Neoarchean to Paleoproterozoic TTG gneisses, supracrustal rocks (metamorphosed sedimentary and volcanic rocks), syn- to post-tectonic granites, and mafic dykes (Liu et al., 2011; Zhao and Zhai, 2013). Many classical indicators of collision tectonics have been found in the TNCO, including linear structural belts defined by strike-slip

ductile shear zones, large-scale thrusting and folding, transcurrent tectonics, shear folds and strong mineral lineations (Trap et al., 2007; Zhang et al., 2007), high-pressure granulites and retrograde eclogites characterized by clockwise metamorphic P–T paths involving near-isothermal decompression (Guo et al., 2002; Zhai et al., 1992, 1995; Zhao et al., 2001). These evidences suggest that the TNCO is a continent–continent collisional belt. On the other hand, SHRIMP metamorphic zircon U–Pb ages, mineral Sm–Nd and Ar/Ar ages, and electron probe microanalysis (EPMA) monazite U–Th–Pb ages from most lithologies of the TNCO reveal that the final collision between the Eastern and Western Blocks occurred at ~1850–1800 Ma (e.g., Guan et al., 2002; Kröner et al., 2005a, 2005b, 2006; Liu et al., 2006; Wan et al., 2006b; Zhao et al., 2002, 2008a).

The Lüliang Complex is located in the western portion of the TNCO, where large amounts of Paleoproterozoic supracrustal rocks and granitoid intrusions are exposed. These supracrustal rock sequences can be divided into four main groups, comprising (from bottom to top) the Jiehekou, Lüliang, Yejishan, and Heichashan or Lanhe Groups (Figs. 1 and 2). These sequences were intruded by the 2375 Ma Gaijiazhuang porphyritic gneiss and the 2182–2151 Ma Guandishan–Chijianling TTG gneiss (Geng et al., 2000, 2004; Liu et al., 2009; Wan et al., 2000, 2006a; Yu et al., 1997b; Zhao et al., 2008b).

The Jiehekou Group is exposed mainly in the northwestern part of the Lüliang area (Fig. 1) and comprises amphibolite- to granulite-facies graphite-bearing pelitic gneiss/schist, quartzite, felsic paragneiss, marble and minor amphibolite/granulite (Wan et al., 2000), which together form part of what has been referred to as the 'khondalite series' in the Chinese literature and is considered to have developed at a passive continental margin (Xia et al., 2009). Based on the ages of the youngest detrital zircons from the khondalite rocks, the Jiehekou Group was formed during the Paleoproterozoic (~2.1–1.9 Ga) (Xia et al., 2009). Furthermore, the zircon U–Pb and Hf isotopic data of these khondalite rocks are similar to those of the khondalite series within the Western Block but different from those of coarse clastic rocks in the Yejishan Group, which suggests that the Jiehekou Group was deposited on the eastern margin of the Western Block and thrust eastward later during collision with the Eastern Block (Liu et al., 2013). In addition, the Lüliang and Jiehekou Groups are clearly different

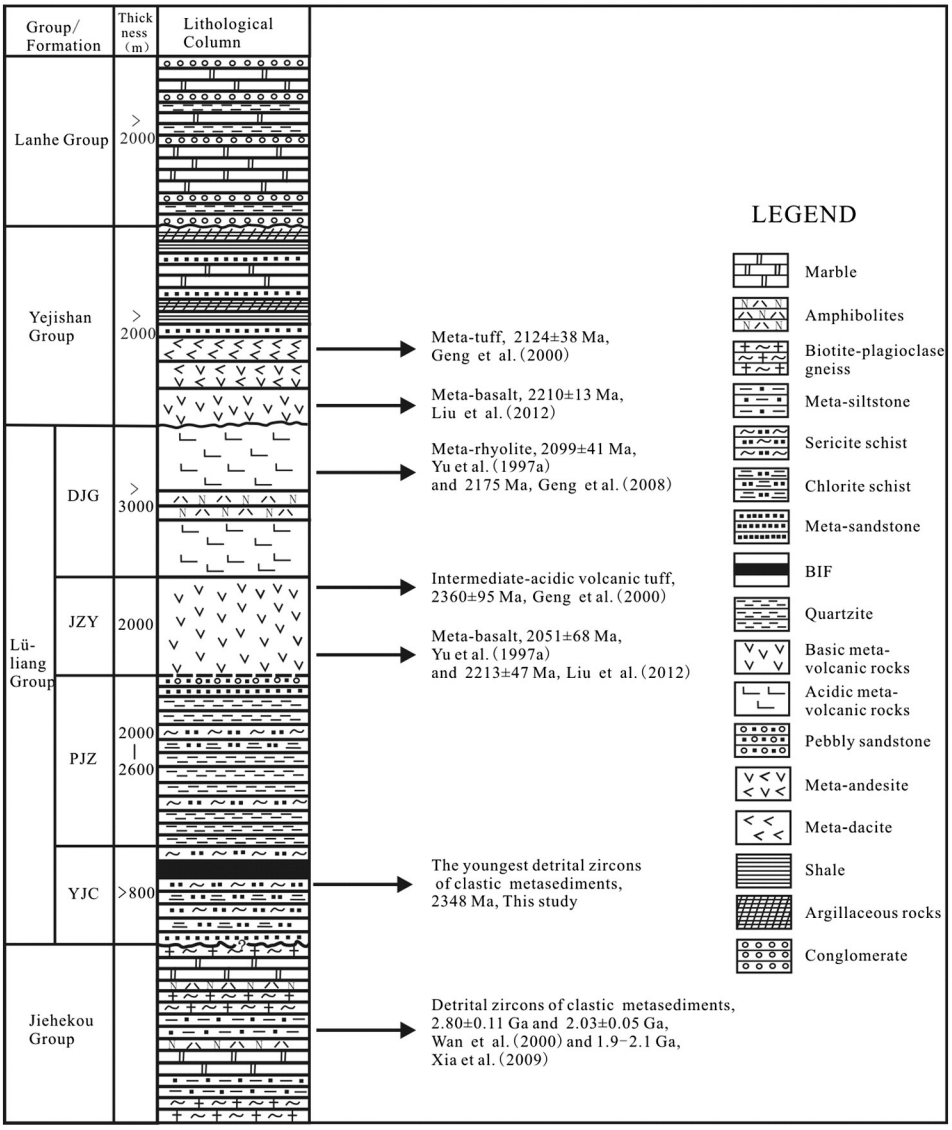

Fig. 2. Stratigraphic column showing group and formation names for different rock assemblages in the Lüliang Complex. Abbreviations for formation names: YJC, Yuanjiacun Formation; PJZ, Peijiazhuang Formation; JZY, Jinzhouyu Formation; and DJG, Dujiagou Formation.
Modified after Tian et al. (1986).

in terms of their rock assemblages, metamorphism, and deformation, indicating that they were likely to be juxtaposed together by subsequent tectonic disturbances.

The Yejishan Group, exposed in the east of the Jiehekou Group, consists of greenschist-facies metamorphosed basalts, andesites, minor dacites in the lower sequence and flysch-like fine-grained sediments in the upper sequence (Liu et al., 2011). The Yejishan Group is unconformably overlain by the Heichashan or Lanhe Group, which is made up of thick-layer subgreenschist-facies metamorphosed conglomerates, quartzites, and dolomitic marbles. Geng et al. (2000) and Liu et al. (2012) obtained U–Pb zircon ages of 2124 ± 38 Ma and 2210 ± 13 Ma from a felsic tuff and a mafic meta-volcanic rock of the Yejishan Group, respectively. And these volcanic rocks display similar geochemical features with a continental margin arc, suggesting that they may have developed in an active continental margin (Liu et al., 2010).

The Lüliang Group, occurring as the west wing of an overturned anticline, strikes roughly S–N and dips to the E. It is distributed only in the Jinzhouyu area and consists predominantly of greenschist- to amphibolite-facies metamorphosed sedimentary rocks with BIFs in the lower sequence and volcanic rocks in the upper sequence (Liu et al., 2012). Regionally, the Lüliang Group is not in direct contact with the Jiehekou Group, but both the two groups are tectonically overlain by the Yejishan and Heichashan Groups. Major lithological assemblages in the Lüliang Group include amphibolites, fine-grained felsic gneisses, schists, BIFs, and tremolite–actinolite marbles. The Lüliang Group is divided into four major units: the lower Yuanjiacun Formation, the middle Peijiazhuang and Jinzhouyu formations, and the upper Dujiagou Formation (Fig. 2). Yu et al. (1997a) obtained single-grained zircon U–Pb ages of 2051 ± 68 Ma and 2099 ± 41 Ma from mafic meta-volcanics in the Jinzhouyu Formation and meta-rhyolites in the Dujiagou Formation, respectively. In addition, three rough ages were reported by Geng et al. (2000, 2008), including zircon U–Pb ages of 2360 ± 95 Ma from the interlayered intermediate-felsic volcanic tuff in the Jinzhouyu Formation and 2175 Ma from the meta-rhyolites in the Dujiagou Formation, and a whole rock Sm–Nd isochron age of 2351 ± 56 Ma for mafic meta-volcanics in the Jinzhouyu Formation. Liu et al. (2001) obtained a whole rock Sm–Nd isochron age of 2464 ± 130 Ma from mafic volcanic rocks in the Jiehekou Group, which they interpreted as the granulite-facies metamorphic age. This age indirectly reveals that the age of the Lüliang Group dates to the Paleoproterozoic, given that its formation age is younger than the granulite-facies metamorphic age but older than the greenschist-facies metamorphic age (~1.85 Ga). Recently, Liu et al. (2012) also reported a U–Pb zircon age of 2213 ± 47 Ma from a mafic volcanic rock in the Jinzhouyu Formation. On the basis of volcanic rock association (meta-basalts and -rhyolites) and their geochemical characteristics in the Lüliang Group, these volcanic rocks are interpreted as having formed in a continental rift basin (Geng et al., 2003; Yu et al., 1997b) or a magmatic arc environment (Liu et al., 2012).

The granitoids, occurring in the Lüliang Complex, have been subdivided into pre-tectonic TTG gneisses, including the 2499 Ma Yunzhongshan, 2375 Ma Gaijiazhuang and 2182–2151 Ma Chijianling–Guandishan gneisses, syn-tectonic gneissic granites represented by the 1832 Ma Huijiazhuang gneissic granite, and post-tectonic TTG gneisses, consisting of the 1800 Ma Luyashan charnockite, 1807 Ma Luchaogou porphyritic granite, and 1800 Ma Tangershang massive granite (Zhao et al., 2008b). The most widespread arc-related magmatic event in the region was the emplacement of the Chijianling–Guandishan granitoid gneisses, of which the tonalitic, granodioritic and monzogranitic gneisses were emplaced at 2199 ± 11 Ma, 2180 ± 7 Ma and 2173 ± 7 Ma, respectively.

2.2. Geology of the Yuanjiacun Formation

The Yuanjiacun Formation exposed in the Yuanjiacun area is a metasedimentary sequence (Fig. 2), which is represented mainly by well-bedded chlorite schists, sericite–chlorite phyllites, sericite schists, quartzite, and minor carbonaceous chlorite schists (Fig. 3a). These metasedimentary are intermittently interbedded with the Yuanjiacun

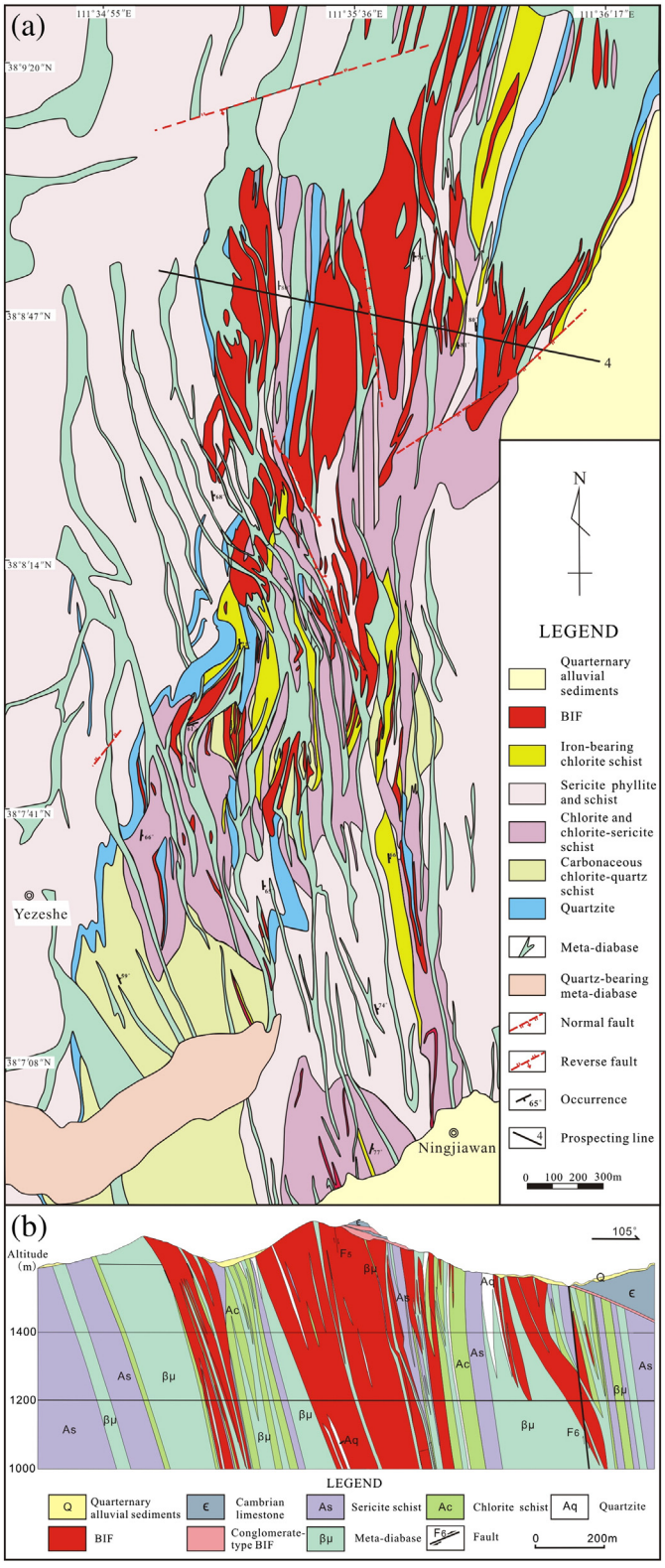

Fig. 3. (a) Geological map of clastic meta-sedimentary rocks in the Yuanjiacun Formation, showing the distribution of the metasediments and associated Yuanjiacun banded iron formation (BIF). (b) Profile of IV prospecting line in the Yuanjiacun area, showing the relationship between the Yuanjiacun BIF and associated meta-sedimentary rocks. Modified from Yao (1993).

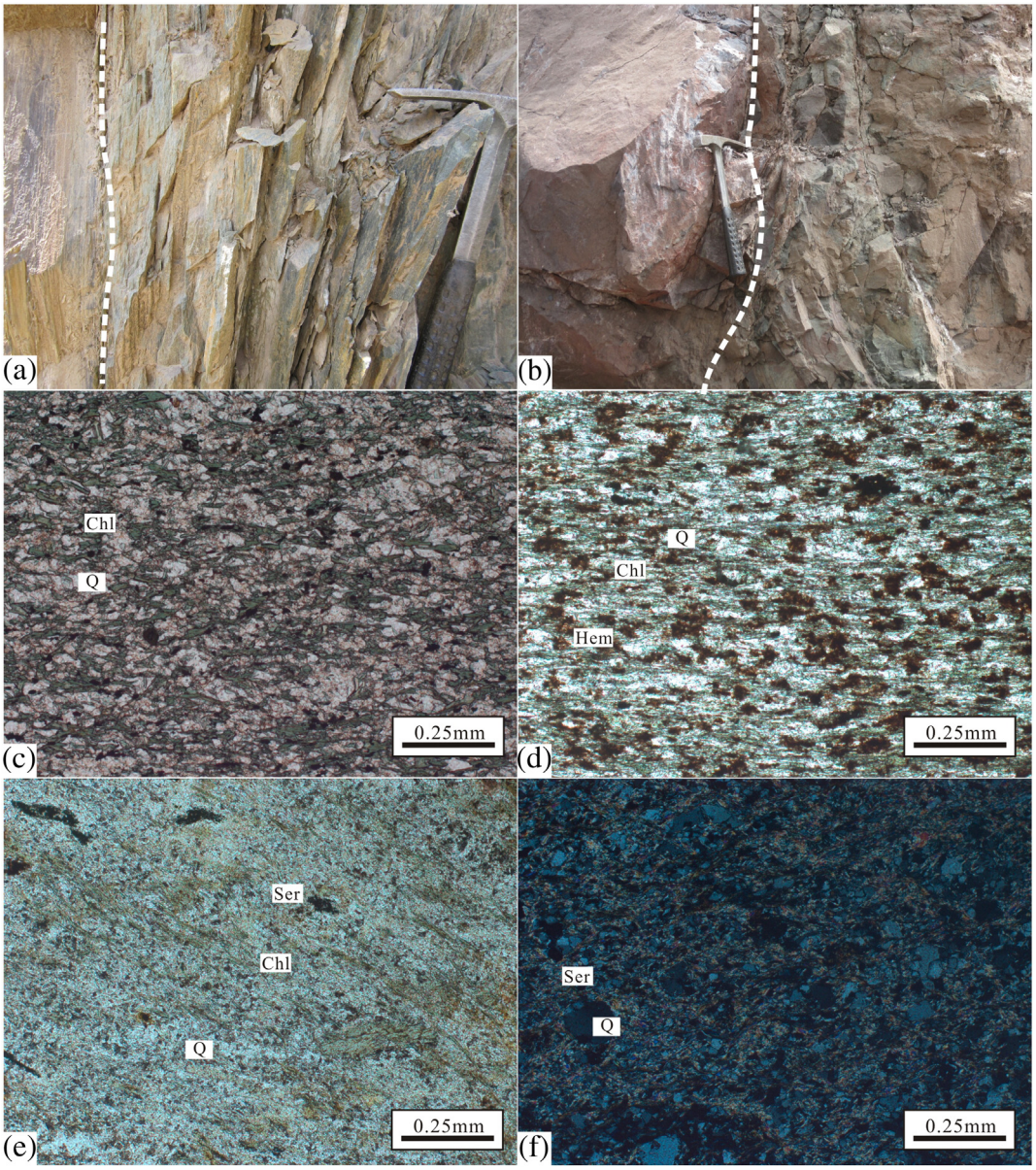

Fig. 4. Field photos of the Yuanjiacun metasediments including (a) and (b). (a) Chlorite schists (right) interlayered with the Yuanjiacun BIF (left) and having a gradual contact with the BIF. (b) Meta-diabase veins (right) penetrate into quartzite (left) with a wavy sharp boundary between them. Photomicrographs showing representative textures and petrographic relationships between the main mineral phases in the Yuanjiacun metasediments, including (c), (d), (e) and (f). (c) Chlorite schists composed mainly of tabular chlorite (Chl) and subhedral–anhedral quartz (Q) grains and chlorite showing a moderate to strong shape preferred orientation (plain-polarized light). (d) Granular hematite (Hem) occurring parallel to the schistosity defined by chlorite in iron-rich chlorite quartz schist (plain-polarized light). (e) Sericite chlorite phyllites consisting predominantly of sericite (Ser), chlorite and quartz and some randomly arranged chlorite aggregates cutting across early foliation defined by tabular chlorite and sericite (plain-polarized light). (f) Very fine-grained sericite schist with angular quartz porphyroblast in a gritty sericite- and quartz-matrix (between crossed polarizers).

BIF (Figs. 3b and 4a). To the south of the Yuanjiacun BIF, however, the degree of metamorphism increases, and the corresponding minerals vary from chlorite–albite schists and sericite quartz schists to grenatite–chlorite schists and amphibolites (Shen et al., 2010). The Yuanjiacun Formation was locally unconformably overlain by the Middle Cambrian limestone (Fig. 3b), at the bottom of which two layers of conglomerate-type BIFs were found approximately 2–14 m apart.

Igneous rocks exposed in the study area consist predominantly of metamorphic diabase with a magmatic crystallization age of ~219 Ma (our unpublished data) and gneissic granite. The former commonly intrudes into the aforementioned meta-sediments as veins with widths varying from several meters to more than 100 m (Fig. 4b). Additionally, it is often dense and massive, characterized by fine grains, weak deformation, and well-developed foliation along the edges. From north to south, the amounts of the diabase increase, the width becomes larger, and the retrograde metamorphism is enhanced. Located in the northern portion of the study area, the stock-like gneissic granite intrudes into the BIF and has a flat or microwave-type contact with the surrounding rocks (Yao, 1993).

3. Petrography

This study is mainly focused on the clastic metasediments associated with the Yuanjiacun BIF. These metasediments consist mainly of chlorite schists, sericite schists, and chlorite–sericite phyllites, which have undergone lower greenschist-facies metamorphism. The chlorite schists and chlorite–sericite phyllites are often interlayered with the BIF and not ubiquitous relative to the sericite schists (Fig. 3a).

The chlorite schists are crumbly, soft, and greenish colored rocks, varying in thickness from tens of decimeters to tens of meters. They

show strong schistosity and comprise chlorite (50–55%), quartz (45–50%), and minor hematite, muscovite, zoisite, and sphene (Fig. 4c). The minor iron-bearing chlorite schists, however, are characterized by high amounts of granular hematite (up to 15%) (Fig. 4d), suggesting continuous deposition of iron in the background. Quartz occurs as subhedral–anhedral grains with 0.1–0.2 mm in size. Occasionally, some quartz grains form larger irregular aggregates. Tabular chlorite (up to 0.3 mm long) commonly shares a moderate shape preferred orientation with strong pleochroism, indicating a high iron content.

The chlorite–sericite phyllites are uncommon, typically dark gray, and display a fine-grained lepido-granoblastic texture and moderately developed foliation. They consist predominantly of sericite (40–45%), quartz (30–35%), and chlorite (25–30%). Occasionally, randomly arranged chlorite aggregates cut across early foliation defined by tabular chlorite and sericite (Fig. 4e).

As the most prominent constituent of the clastic metasediments, the sericite schists are situated mainly in the west of the studied area (Fig. 3a). They are faintly laminated (<1 mm) and are composed predominantly of sericite (60–65%) and quartz (35–40%). The rock is very fine-grained with few porphyroblasts of quartz scattered in a matrix of sub-angular quartz and sericite (Fig. 4f). The main foliation is commonly defined by sericite flakes. Whether the fine-grained mica is an

Table 1
Average major and trace element compositions of the metasediments of the Yuanjiacun Formation and other Precambrian sediments from international references[a].

Element	Low-Al meta-pelite	High-Al meta-pelite[b]	Meta-arenite	Proterozoic cratonic shales (1)	Proterozoic graywackes (1)	PAAS (2)	NASC (3)	Upper continental crust (4)
SiO_2	48.0	66.9	75.1	63.1	66.1	62.8	64.8	66.6
TiO_2	1.64	0.61	0.62	0.64	0.77	1.00	0.70	0.64
TFe_2O_3	23.5	5.39	3.29	5.65	5.80	6.50	5.67	5.04
Al_2O_3	13.4	17.4	13.4	17.5	15.0	18.9	16.9	15.4
MnO	0.14	0.02	0.01			0.11	0.06	0.10
MgO	5.51	1.22	1.16	2.20	2.10	2.20	2.86	2.48
CaO	0.96	0.23	0.13	0.71	2.60	1.30	3.63	3.59
Na_2O	1.10	0.20	0.18	1.06	2.80	1.20	1.14	3.27
K_2O	0.25	5.28	4.23	3.62	2.50	3.70	3.97	2.80
P_2O_5	0.37	0.14	0.06	0.12	0.14	0.16	0.13	0.15
Ni	58.6	26.4	18.5	52.0	45.0	55.0	58.0	47.0
Cr	98.5	122	245	115	80.0	110	125	92.0
Sc	27.2	14.1	7.96	17.0	17.0	16.0	15.0	14.0
V	224	121	46.3	100	140	150	130	97.0
Cs	0.11	5.32	3.12			15.0	5.16	4.90
Ba	70.8	940	583	642	600	650	636	628
Rb	4.63	170	109	165	80.0	160	125	82.0
Sr	35.0	68.1	39.0	108	240	200	142	320
Hf	4.31	8.90	6.34	5.20	4.20	5.00	6.30	5.30
Zr	166	299	256	196	148	210	200	193
Y	23.6	29.8	12.5	35.0	27.0	27.0	35.0	21.0
Ta	0.65	1.21	0.57	1.40	0.80	1.28	1.12	0.90
Nb	10.1	13.8	8.72	16.8	10.0	19.0	13.0	12.0
Ga	19.8	24.4	16.7					17.5
Cu	15.1	25.9	9.72					28.0
Zn	95.2	20.2	23.3					67.0
Pb	1.68	4.29	6.70	27.0	10.0	20.0	20.0	17.0
Th	3.83	19.6	6.79	14.3	9.00	14.6	12.3	10.5
U	0.87	3.72	1.41	3.40	1.70	3.10	2.70	2.70
La	27.3	22.1	36.7	38.0	28.0	38.2	31.1	31.0
Ce	52.9	43.4	70.9	81.7	60.0	79.6	67.0	63.0
Pr	6.82	5.83	8.44			8.83		7.10
Nd	26.1	23.8	27.2	37.5	26.0	33.9	30.4	27.0
Sm	5.22	5.25	4.07	6.68	4.90	5.55	5.98	4.70
Eu	1.52	1.07	1.01	1.32	0.93	1.08	1.25	1.00
Gd	4.66	5.02	3.06	5.60	4.34	4.66	5.50	4.00
Tb	0.75	0.94	0.43	0.90	0.66	0.77	0.85	0.70
Dy	4.65	6.19	2.47			4.68	5.54	3.90
Ho	0.99	1.34	0.50			0.99		0.83
Er	2.79	3.84	1.44			2.85	3.28	2.30
Tm	0.42	0.58	0.23			0.41		0.30
Yb	2.75	3.73	1.52	2.86	2.20	2.82	3.11	2.00
Lu	0.42	0.57	0.24	0.48	0.38	0.43	0.46	0.31
K_2O/Na_2O	0.23	26.4	24.0	3.42	0.89	3.08	3.48	0.86
Al_2O_3/TiO_2	8.18	28.5	21.9	27.3	19.5	18.9	24.1	24.1
SiO_2/Al_2O_3	3.58	3.84	5.64	3.61	4.41	3.32	3.83	4.32
Th/Sc	0.14	1.39	0.86	0.84	0.53	0.91	0.82	0.75
La/Sc	1.00	1.57	4.63	2.22	1.65	2.38	2.07	2.21
Th/U	4.39	5.26	4.82	4.21	5.29	4.71	4.56	3.89
Zr/Sc	6.09	21.2	32.0	11.5	8.71	13.1	13.3	13.8
ΣREE	137	124	158			185		148
Eu/Eu*	0.94	0.64	0.87	0.66	0.62	0.65	0.67	0.71
$(La/Yb)_N$	7.13	4.34	17.6	9.53	9.13	9.72	7.17	11.1
$(La/Sm)_N$	3.38	2.87	6.16	3.67	3.69	4.44	3.36	4.26
$(Gd/Yb)_N$	1.40	1.11	1.69	1.62	1.63	1.37	1.46	1.65
CIA	87	73	72	72	56	70	68	53
CIW	90	74	73	76	67	76	73	65

[a] References: (1) Condie (1993); (2) McLennan (1989); (3) Gromet et al. (1984); (4) Rudnick and Gao (2003).
[b] Sample WY12-7 is excluded due to an abnormally high amount of LREE.

alteration product of feldspars is unknown due to the fine-grained texture.

4. Results

4.1. Geochemical and Sm–Nd isotopic results

Whole-rock major, trace and REE elements, and Nd isotopic compositions of representative samples from the metasediments of the Yuanjiacun Formation are given in Appendix Tables 1 and 2. Table 1 presents some universal reference compositions including the Proterozoic graywackes and cratonic shales (Condie, 1993), PAAS (post-Archean Australian shale; McLennan, 1989), NASC (North American shale composite; Gromet et al., 1984) and UCC (upper continental crust; Rudnick and Gao, 2003).

4.1.1. Major elements

On the geochemical classification diagram of Herron (1988) (Fig. 5), the protolith of the chlorite schists and chlorite–sericite phyllites is discriminated as shale and Fe-shale, while the protolith of the sericite schists straddles the graywacke and arkose fields.

The meta-pelites show an obviously wide range for almost all major element contents, including SiO_2 (40.3–67.8%), TiO_2 (0.43–2.65%), Al_2O_3 (12.4–18.4%), TFe_2O_3 (total Fe as Fe_2O_3) (5.21–32.3%) and K_2O (0.06–5.72%). The meta-pelites can be classified into two distinct groups in terms of geochemical compositions: low-Al and high-Al meta-pelites. The former is characterized by higher contents of TFe_2O_3, MgO, CaO, TiO_2 and lower Al_2O_3 and SiO_2 relative to the latter. Conversely, the meta-arenites exhibit a restricted compositional range, such as SiO_2 (71.7–78.3%), TiO_2 (0.48–0.67%), and Al_2O_3 (11.9–14.3%). By comparison, the meta-pelites are enriched in TFe_2O_3, Al_2O_3, MgO, and CaO and depleted in SiO_2 and K_2O relative to those of the meta-arenites.

The high-Al meta-pelites are exceptionally enriched in Al_2O_3 (an average of 17.4%), reflecting the control of their composition by aluminous clay minerals, whereas the low-Al meta-pelites and meta-arenites are relatively low in alumina (an average of 13.4%), suggesting a low clay content. Compared to the international standards (e.g., PAAS, NASC, and UCC), the low-Al meta-pelites are characterized by high contents of TFe_2O_3 due to their close relationship with the Yuanjiacun BIF, and the average Al_2O_3 contents in the low-Al meta-pelites and meta-arenites are lower than in UCC, likely suggesting their distinct source materials.

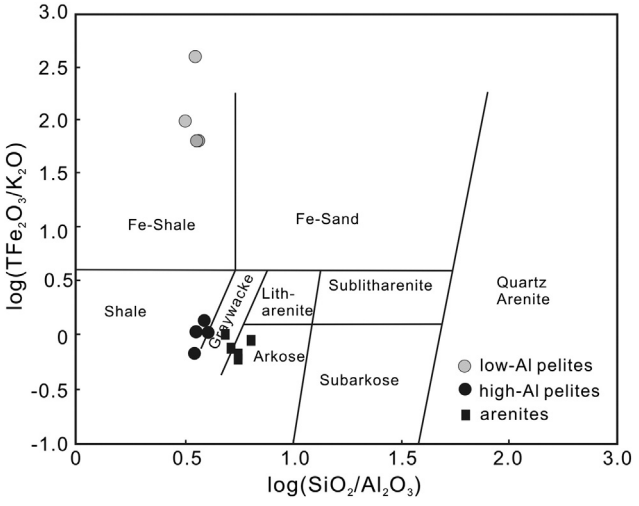

Fig. 5. Geochemical classification of the Yuanjiacun metasediments using the $\log(SiO_2/Al_2O_3)$ vs. $\log(TFe_2O_3/K_2O)$ diagram (Herron, 1988). White and black solid circles represent low-Al and high-Al pelites, respectively. Black solid squares represent arenites.

At the same time, the high-Al meta-pelites have considerably high Al_2O_3/SiO_2 values due to their unique high contents in alumina. The high K_2O/Na_2O ratios found in the meta-arenite and high-Al meta-pelite samples most likely reflect secondary addition of potassium (K-metasomatism) (Fedo et al., 1995). In addition, the SiO_2/Al_2O_3 values of the meta-pelite samples vary from 3.25 to 4.12, similar to that of igneous rocks (3–5), reflecting the slightly immature nature of these metasediments. In contrast, the meta-arenites display higher SiO_2/Al_2O_3 values (>5), providing evidence of sedimentary maturation (Roser et al., 1996). The abundance of CaO in these metasediments is very low, always less than 1.4% and typically less than 0.6%.

Variations in the major element geochemistry of the metasedimentary rocks are shown on Harker diagrams (Fig. 6). The meta-pelites and meta-arenites are discriminated into two distinct populations in all diagrams; however, the whole samples show variable but still negative correlations of SiO_2 against all major oxides except Al_2O_3, K_2O, and Na_2O. SiO_2 exhibits positive and negative correlations with Al_2O_3 for the meta-pelites and meta-arenites, respectively. The broad scatter between SiO_2, K_2O, and Na_2O may be attributed to high Na and K mobility during later metamorphism. The strong correlation of Al_2O_3 and TiO_2 ($r = -0.81$ and 0.94, respectively) suggests that Ti is manly concentrated in phyllosilicates (Condie et al., 1992). Considering that TFe_2O_3 (or MgO) contents do not exhibit a correlation with Al_2O_3 for the meta-pelites, the strong correlation between TFe_2O_3 and TiO_2 ($r = 0.89$) can be attributed to iron oxides rather than chlorite in these samples.

4.1.2. Large ion lithophile elements (LILEs)

The Rb, Ba, K, and Sr concentrations normalized to the UCC values of Rudnick and Gao (2003) are given in Fig. 7a and b. The meta-arenites and high-Al meta-pelites show enrichment in Rb and K. Ba contents for the meta-arenites scatter around the UCC values, while for the meta-pelite samples, the Ba enrichment is coupled with the enrichment of Rb. Sr is variably depleted in all samples, which is in line with the general relative depletion of Ca, implying that plagioclase in the source material of these metasediments was decomposed during weathering.

4.1.3. High field strength elements (HFSEs)

The HFSEs are incompatible during most magma crystallization and anatectic processes (Feng and Kerrich, 1990), therefore, they are more enriched in felsic than mafic rocks. The meta-pelites are enriched in Ti and Y when compared to the meta-arenites (Fig. 7a and b). The average Zr content (256 ppm) for the meta-arenites is higher than those of the UCC (193 ppm), indicating a preferential accumulation of detrital zircon and the maturity nature (El-Bialy, 2013). Nevertheless, preferential accumulation of iron oxide minerals (e.g., hematite) likely occurs in the meta-pelites due to the higher Ti concentrations (2662–16754 ppm) than that of the UCC (3765 ppm). The low-Al meta-pelites and meta-arenites are depleted in Th and U relative to the UCC. Zr–Hf and Nb–Ta show high positive correlations for all the samples, as expected from their similar geochemical feature.

4.1.4. Transition elements

This group of elements includes Ni, Cr, Sc and V, which are regarded as compatible ferromagnesian trace elements. Ni is obviously depleted in both of the high-Al meta-pelite and meta-arenite samples (average of 26.4 and 18.5 ppm, respectively) relative to UCC (47 ppm), NASC (58 ppm) and PAAS (55 ppm). The Cr contents of the meta-arenite samples are exceptionally higher than that of other meta-sediments mentioned in Table 1. However, the low-Al meta-pelite samples have evidently higher concentrations of Sc and V compared to that of the aforementioned references, indicating the presence of mafic components in the source of these metasediments (Wang et al., 2012).

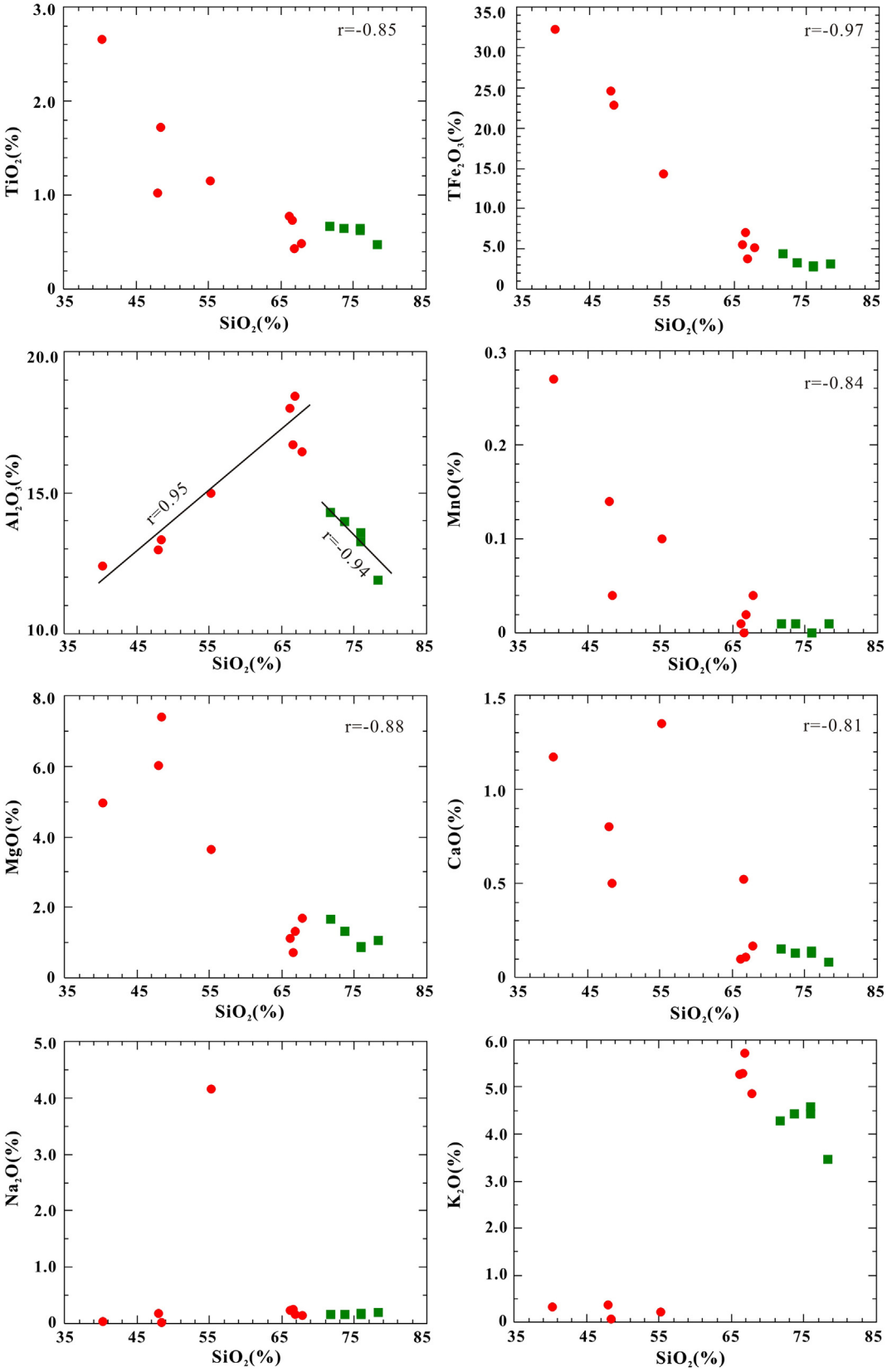

Fig. 6. Harker variation diagrams of major oxides versus SiO_2 for the Yuanjiacun metasediments. Note the grouping of the meta-pelites and meta-arenites into two populations on all diagrams. Solid circles and squares represent meta-pelites and meta-arenites, respectively. r is the correlation coefficient.

4.1.5. Rare earth elements (REEs)

One of the meta-pelite samples (WY12-7) displays a high light REE content, such as La (325.29 ppm). This variability is likely to be attributed to the accumulation of accessory minerals such as zoisite in this sample. Therefore, this sample is excluded from the discussion below.

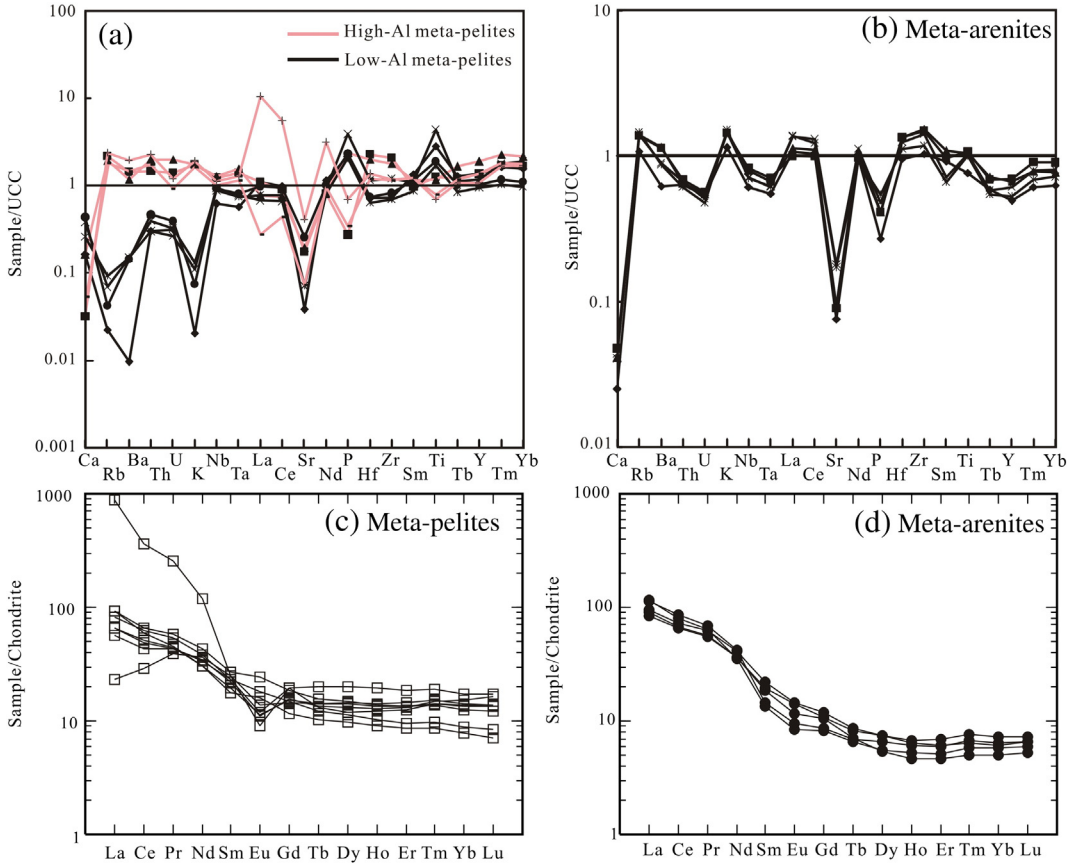

Fig. 7. Upper Continental Crust (UCC; Rudnick and Gao, 2003) normalized spider diagrams of the meta-pelites (a) and meta-arenites (b). Chondrite-normalized REE patterns for the meta-pelites (c) and meta-arenites (d).
Chondrite normalization values are from Sun and McDonough (1989).

All samples exhibit variable abundances of total REE (REE) (average of 137, 124, and 158 ppm, respectively), which are comparable to those of the UCC and PAAS (Table 1). The chondrite-normalized REE patterns of the metasediments (Fig. 7c and d) are generally sub-parallel, LREE-enriched with distinct Eu anomalies. The heavy REEs are weakly fractionated with slightly inclined to flat patterns. The meta-arenites are obviously enriched in REE and have a slightly higher degree of LREE fractionation ($(La/Yb)_N = 12.3–21.2$) with weaker negative Eu anomalies ($Eu/Eu^* = 0.82–0.97$) relative to those of the high-Al meta-pelites (Table 1). Moreover, the negative Eu anomalies in the high-Al meta-pelites are similar to those of the UCC, NASC, and PAAS (0.71, 0.67, and 0.65, respectively). In addition, the Eu anomalies of the low-Al meta-pelites have a large range, varying from 0.59 to 1.12.

4.1.6. Nd isotopes

ε_{Nd} values are calculated at 2300 Ma, which represents the approximate age of these metasediments (see under Discussion). All samples have $^{147}Sm/^{144}Nd$ values ranging from 0.10 to 0.13, similar to the value of UCC (0.118; Jahn and Condie, 1995), indicating little differentiation of Sm/Nd during sedimentation and source magmatic processes. Data for all metasedimentary rocks yield T_{DM} model ages between 2.9 and 2.5 Ga (Appendix Table 2). The $\varepsilon_{Nd}(t)$ values of the low-Al meta-pelites are consistently positive, ranging from 0.4 to 2.9, whereas those of the high-Al meta-pelites range from −3.7 to −0.5. The meta-arenites have also negative $\varepsilon_{Nd}(t)$ values varying from −4.3 to −1.5. The significant positive $\varepsilon_{Nd}(t)$ values of low-Al meta-pelites are attributed to more juvenile materials in their source areas (see under Discussion).

4.2. Detrital zircon U–Pb ages

Detrital zircon U–Pb ages for the meta-arenite (sericite schist) sample are presented in Appendix Table 3. The zircons are mainly subrounded or subhedral prismatic in shape with variable grain size (30–110 μm). Most grains are light brown in color and have obvious magmatic oscillatory zoning (Appendix Fig. 1). These features, together

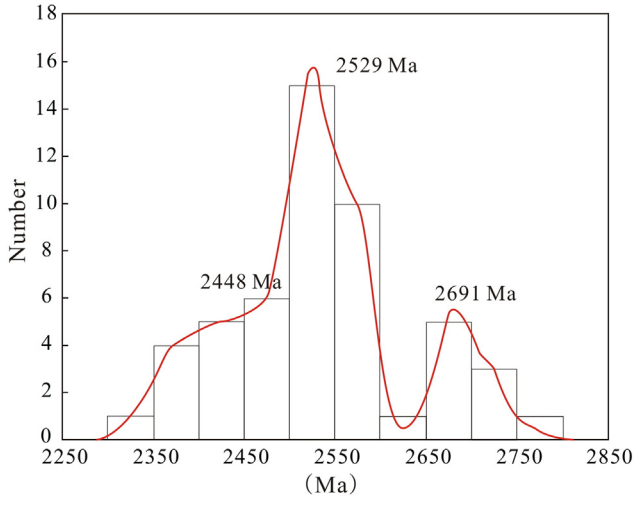

Fig. 8. Binned frequency histogram of detrital zircons for the Yuanjiacun meta-arenites.

with their high Th and U contents and Th/U ratios (>0.4), point to a magmatic origin.

Representative concordant and nearly concordant zircons with age discordance of less than 15% are reliable enough that they were used in binned frequency histograms. All 51 analyses are plotted on or near the Concordia curve and display a wide range of $^{207}Pb/^{206}Pb$ ages, from 2348 to 2757 Ma. The $^{207}Pb/^{206}Pb$ age spectrum (Fig. 8) displays a primary peak at 2529 ± 10 Ma, a shoulder at 2448 ± 20 Ma, and a minor peak at 2691 ± 28 Ma.

5. Discussion

5.1. Depositional age of the Yuanjiacun metasediments

The depositional age of the Yuanjiacun Formation metasediments has not been well constrained due to the absence of volcanogenic interbeds suitable for dating. Previously published data, including zircon U–Pb ages of the meta-volcanic rocks from the overlying Jinzhouyu and Dujiagou formations, have been used to infer that the volcano-sedimentary rocks of the Lüliang Group were deposited between 2.3 and 2.1 Ga (Fig. 2) (Geng et al., 2000, 2008; Liu et al., 2012; Yu et al., 1997a). In particular, Liu et al. (2012) used the LA–ICP-MS U–Pb zircon dating technique to determine that the mafic meta-volcanic rocks in the Jinzhouyu Formation were formed at 2213 ± 47 Ma and metamorphosed at ~1832 Ma, suggesting that the underlying Yuanjiacun Formation may have been deposited some time before 2213 Ma.

Most of the detrital zircon grains from the Yuanjiacun meta-arenites show subhedral shapes and oscillatory zoning with Th/U values greater than 0.4, suggesting a magmatic origin and showing no evidence of metamorphic resetting or recrystallization after their deposition. Sedimentary rocks associated with the Yuanjiacun BIF experienced greenschist facies metamorphism (Yu et al., 1997b), which precludes the possibility that the U–Th–Pb systems in the detrital zircons have been reset. Therefore, the obtained youngest ages can place further and reliable constraints at the maximum depositional time. The youngest group of detrital zircons consists of five grains (Appendix Table 3), which defines a weighted average age of 2384 ± 45 Ma, slightly older than the single-grain youngest age of 2348 ± 78 Ma. Thus, the age of ~2350 Ma represents the best estimate of the maximum depositional age for the protolith of the metasedimentary sequences.

Taking the above-mentioned into account, the depositional age of the Yuanjiacun Formation can be constrained to the period between 2350 and 2213 Ma.

5.2. Element mobility

Because the metasediments associated with the Yuanjiacun BIF have undergone greenschist-facies metamorphism, it is important to evaluate the effect of metamorphism on the mobility of major and trace elements and isotopic composition. Many elements in metamorphic rocks are mobilized by interaction with fluids, solid-state diffusion and melt generation (Rollinson, 1993). However, Rollinson (1993) argued that, at a scale of several centimeters or more, the effect of solid-state diffusion of elements within rocks is negligible and that the main concern is fluid-controlled mobility. Several studies have reported that element ratios of metasedimentary rocks, such as K_2O/Na_2O and TiO_2/Al_2O_3, have not been generally affected by high-grade regional metamorphism (Fralick and Kronberg, 1997; Roser and Korsch, 1986). Roser and Korsch (1986) further suggested that using such a ratio, in conjunction with trace element data, can prove useful for discrimination of provenance and tectonic setting.

High field strength elements such as Th, Zr, Hf, Ti, Nb, Ta, and REEs, are often considered to be relatively immobile elements (McLennan, 1989; Pearce, 1996; Taylor and McLennan, 1985), because these elements are not significantly modified during chemical weathering and diagenesis such that provenance information may not be lost. Similarly, whole-rock Sm–Nd isotope systems can apparently remain undisturbed even after severe metamorphism and deformation (Barovich and Patchett, 1992). Thus, selected trace elements and Nd isotopic data are commonly used as a tool in sedimentary provenance.

5.3. Source-area weathering

The chemical composition of clastic sediments is mainly controlled by a number of geological factors, including source rock composition, the intensity of weathering, the rate of sediment supply, and sorting (both textual and mineralogical) during transportation and deposition, and finally post-depositional weathering (Cullers et al., 1997; McLennan, 1989; Roddaz et al., 2006). Effects of these processes have to be considered before drawing conclusions on the nature of source rocks and tectonic setting of the region as inferred from the geochemistry of clastic sediments.

Weathering in the source areas would result in relative depletion of alkaline elements and LILEs and the enrichment of TiO_2 and Al_2O_3 in clastic sedimentary rocks (McLennan et al., 1993; Nesbitt et al., 1980). The most widely used chemical index to quantitatively measure the intensity of source-area weathering is the Chemical Index of Alteration (CIA; Nesbitt and Young, 1982) or the Chemical Index of Weathering (CIW; Harnois, 1988) (Appendix Table 1). The CIA index measures the degree of weathering of feldspars relative to unaltered protolith and is defined as: $CIA = [Al_2O_3 / (Al_2O_3 + CaO^* + Na_2O + K_2O)] \times 100$ (molar proportions), where CaO^* represents the CaO content in the silicate fraction. We do not have CO_2 data in our analyses to correct Ca in carbonates. To calculate CaO^*, we have accepted the value of CaO if $CaO \leq Na_2O$; for $CaO > Na_2O$, we assumed that the concentration of CaO equals Na_2O (Bock et al., 1998). Generally, unweathered basalts and granitoids are characterized by CIA values of 30–45 and 45–55, respectively, while average shales have CIA values of 68 (NASC) to 70 (PAAS). The low-Al meta-pelites have large CIA values (up to 99), whereas CIA values for the high-Al meta-pelites and meta-arenites vary between 71 and 74. This would indicate that the source rocks of the low-Al meta-pelites underwent severe chemical weathering, whereas those of the high-Al meta-pelites and meta-arenites have suffered moderate chemical weathering. In addition, the Plagioclase Index of Alteration (PIA) is similar to CIA, but is not affected by K-metasomatism (Fedo et al., 1995). The studied metasediments display generally high PIA ratios (>90), reflecting relatively intense weathering of their sources.

Data are plotted on a ternary diagram of molecular proportions A (Al_2O_3)–CN ($CaO^* + Na_2O$)–K (K_2O), where CaO^* is the CaO in the silicate fraction only (Fig. 9a). Several idealized mineral compositions are plotted for reference (Nesbitt and Young, 1984). Plots of the studied samples display two distinct trends. The low-Al meta-pelite samples define a trend parallel to the A–CN axis and extending towards the A apex, essentially similar to the trends for surface weathering of boninite. This confirms that the low-Al meta-pelites are extensively weathered relative to other samples. Additionally, the high-Al meta-pelites and meta-arenites plot along the A–K boundary between idealized muscovite and biotite composition. The apparent enrichments in K are attributed to hydrothermal or other alterations, apart from weathering.

Th/U ratios for sedimentary rocks generally increase with increasing degrees of weathering due to oxidation and the loss of uranium. In general, Th/U values greater than 4.0 would point to intense weathering in the source area or sediment recycling (McLennan et al., 1993, 1995). Plots of the metasediments on the Th/U vs. Th diagram (Fig. 9b) reveal that almost all the samples have Th/U ratios higher than the upper crust value and follow the previous weathering trend (McLennan et al., 1993), suggesting that these rocks have suffered intense weathering.

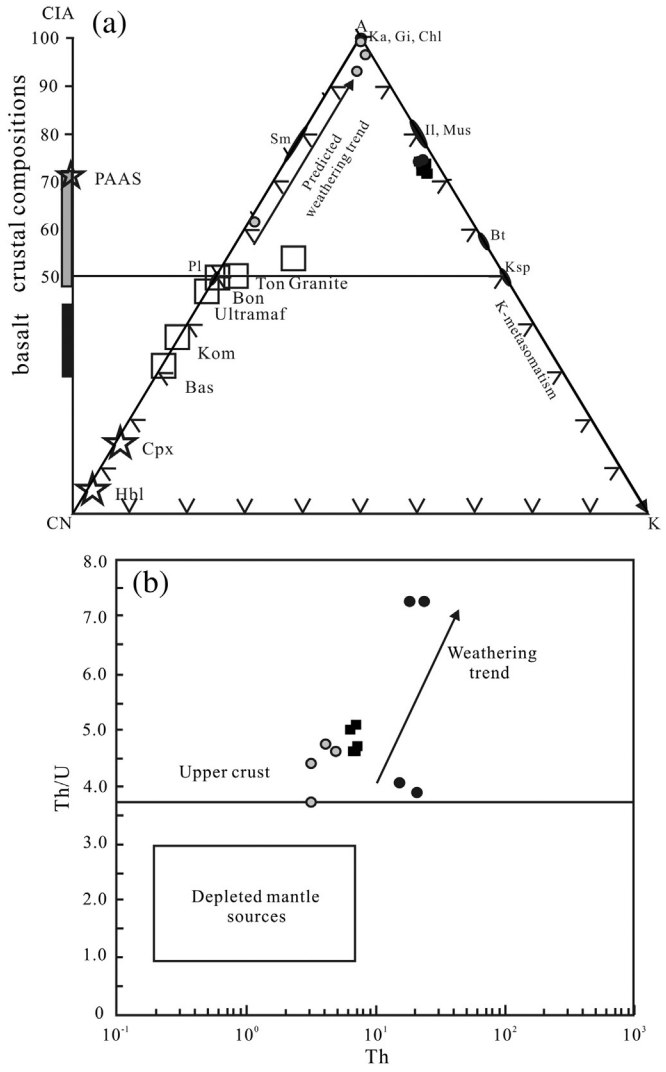

Fig. 9. (a) Ternary plot of molecular proportions Al_2O_3(A) − CaO* + Na_2O(CN) − K_2O(K) (Nesbitt and Young, 1989) for the metasediment samples with Chemical Index of Alteration (CIA) scale. Solid arrows represent weathering trends of these metasediments. Also shown are idealized mineral and igneous rock compositions: Ka = kaolinite, Gi = gibbsite, Chl = chlorite, Il = illite, Mus = muscovite, Bt = biotite, Ksp = K-feldspar, Sm = smectite, Pl = plagioclase, Cpx = clinopyroxene, Hbl = Hornblende, Bas = basalt, Kom = Komatiite, Ultramafic = unltramafic ultramafic rock, Bon = boninite, and Ton = tonalite. (b) Plot of Th/U ratios vs. Th abundances for metasedimentary rocks from the Yuanjiacun Formation (McLennan et al., 1993). Symbols are the same as in Fig. 5.

5.4. Sedimentary processes and maturation

Sedimentary processes like sorting are of particular importance in modifying the mineral abundances and consequently the concentrations of specific elements. Specifically, sedimentary sorting is responsible for the systematic fractionation between SiO_2 (quartz) and Al_2O_3 (clays), as well as between Zr (zircon) and other minor or trace elements that are preferentially retained in the fine-grained fraction (Garcia et al., 1994). The variability of the $100TiO_2/Zr$ (wt.%/ppm) ratio is a sensitive indicator of the intensity of sorting (Garcia et al., 1994). The high-Al meta-pelites and meta-arenites have $100TiO_2/Zr$ ratios lower than 0.33, coupled with the corresponding Al_2O_3/SiO_2 ratios close to 0.23, pointing to geochemical maturity and consequently greater degree of sedimentary recycling.

Sorting may also play a significant role in favoring plagioclase accumulation in sands, which results in a decrease of the negative Eu anomaly (McLennan et al., 1993). In the absence of abundant plagioclase, there is no systematic Eu enrichment in sands over associated muds (Bhatia, 1985). In our study, the high-Al meta-pelites have lower negative Eu anomalies than their associated meta-arenites, which confirms the presence of plagioclase concentration due to sand sorting.

A plot of Th/Sc versus Zr/Sc can reflect the extent of sedimentary sorting and recycling (Fig. 10a) (McLennan et al., 1990). The Th/Sc ratio is an indicator of chemical differentiation, while the Zr/Sc ratio measures the degree of sediment recycling. First-cycle sediments show a simple positive correlation between Th/Sc and Zr/Sc, whereas additionally recycled sediments usually show a more rapid increase in Zr/Sc than in Th/Sc. The low-Al meta-pelite samples follow the magmatic compositional variation, but all of the meta-arenite and high-Al meta-pelite samples displace towards higher Zr/Sc ratios (>10), suggesting some degree of sediment reworking and sorting. In addition, zircon preferentially incorporates HREE relative to LREE, resulting in HREE enrichment and low $(La/Yb)_N$. Therefore, a negative correlation between Zr and $(La/Yb)_N$ would be expected if zircon concentrates. Such a relationship exists for the meta-arenites ($r = -0.71$), indicating that the preferential accumulation of zircon occurs. Moreover, all samples from the mete-arenites and high-Al meta-pelites have higher Zr and lower Sr contents than those of the UCC, reflecting a greater degree of recycling for these metasediments (Asiedu et al., 2004; Mader and Neubauer, 2004).

Roser and Korsch (1988) developed a convenient method for determining the provenance of clastic sediments (Fig. 10b). Three low-Al

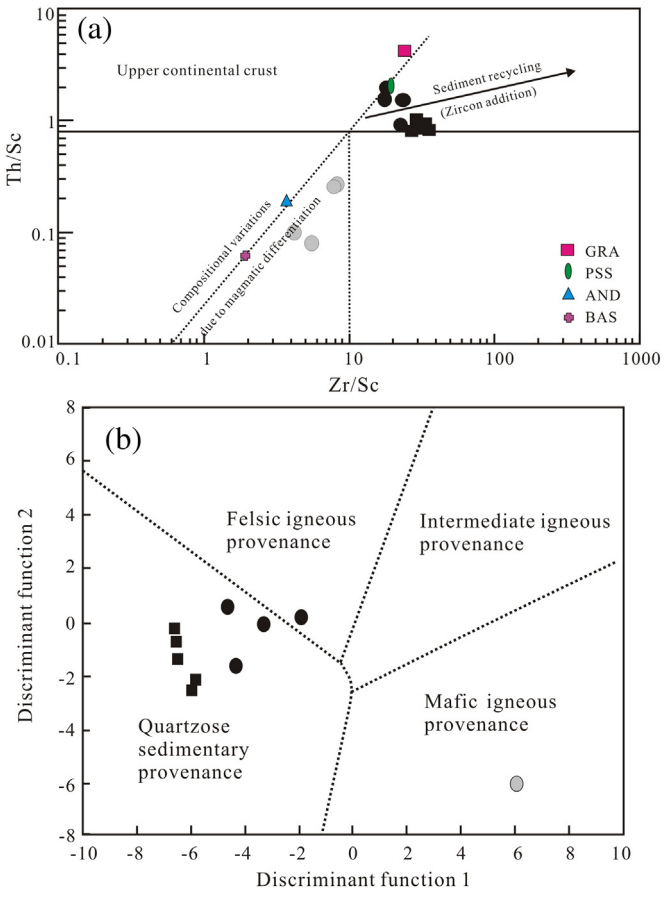

Fig. 10. (a) Plot of Th/Sc versus Zr/Sc (after McLennan et al., 1993) for the Yuanjiacun metasediments. Average source rock compositions are of Proterozoic age (after Condie, 1993). BAS, basalt; AND, andesite; GRA, granite; and PSS, Proterozoic sandstone. (b) Discriminant function diagram for the provenance signatures of the meta-pelites and meta-arenites using major elements (after Roser and Korsch, 1988). D1 = $-1.773TiO_2 + 0.607Al_2O_3 + 0.76\ Fe_2O_3$ (total) − 1.5MgO + 0.616CaO + $0.509Na_2O - 1.224K_2O$ − 9.09; D2 = $0.445TiO_2 + 0.07Al_2O_3 - 0.25Fe_2O_3$ (total) − 1.142MgO + 0.438CaO + 1.475 $Na_2O + 1.426\ K_2O$ − 6.861. Symbols are the same as in Fig. 5.

meta-pelite samples are not plotted due to high contents of iron. They are plotted in the mafic igneous provenance field, suggesting that a significant mafic composition contributes to their source area. Most high-Al meta-pelite and meta-arenite samples are plotted in the quartzose sedimentary provenance field. This field comprises recycled mature sediments containing polycyclic quartzose detritus, denoting that these metasediments were mainly derived from a pre-existing sedimentary terrane with little contribution from magmatic sources.

The Index of Compositional Variability (ICV; Cox et al., 1995) has been applied to mudrocks as a measure of compositional maturity. Compositionally immature mudrocks that contain a high proportion of nonclay silicate minerals, or that are rich in clay minerals such as montmorillonite and sericite, will have high values on this index, whereas compositionally mature mudrocks, poor in nonclay silicates or dominated by minerals such as those of the kandite family, will have low values. With the exception of the low-Al meta-pelites, other metasediment samples have low ICV values (<1), indicating that they are compositionally mature and may be either derived from tectonically quiescent or cratonic environments where sediment recycling is active, or produced by intense chemical weathering of first-cycle material.

5.5. Provenance

The grain size of our collected sediments ranges from mud to fine sand, which are more likely to have a mineralogical and chemical composition similar to their sources than coarser sand fractions (Cullers, 1988, 1994b). The Al_2O_3/TiO_2 ratio is commonly used to indicate the provenance of sedimentary rocks. Hayashi et al. (1997) demonstrated that Al_2O_3/TiO_2 ratios of sandstones and mudstones are fundamentally identical to those of their source rocks. In most cases, the fractionation of Al and Ti is insignificant between silts/shales and their parent rocks, probably because most Ti in weathered rocks occurs as a chemical constituent of chlorite (and other clays) and/or as minute Ti–Fe oxide inclusions in these silicate minerals, rather than as separate ilmenite grains (Hayashi et al., 1997). The Al_2O_3/TiO_2 ratio of the low-Al meta-pelites ranges from 4.68 to 13.0, indicating that they are derived predominantly from mafic sources, whereas the ratio for the high-Al meta-pelites and meta-arenites varies from 20.4 to 42.8, suggesting that they are derived mainly from felsic rocks. The A–CN–K triangular plot (Fig. 9a) can also be used to constrain the original compositions of source rocks (Fedo et al., 1995). The weathering trend of low-Al meta-pelite samples is parallel to the A–CN line, indicating that they seem to be derived from more compositionally limited igneous sources (largely mafic).

Trace elements, such as Zr, Nb, Hf, Ta, Th, U, and Sc, have proven useful in discriminating among sedimentary sources (McLennan et al., 1990, 1993; Taylor and McLennan, 1985). The studied low-Al meta-pelites have obviously higher amounts of compatible ferromagnesian trace elements (i.e., V, Sc), inferring more mafic rocks in the source area (Floyd et al., 1991). Moreover, ratios such as Eu/Eu*, La/Sc and Th/Sc are radically different in mafic and felsic source rocks and can be used to accurately constrain the provenance of sedimentary rocks (Taylor and McLennan, 1985). These ratios of the high-Al meta-pelite and meta-arenite samples are similar to those for sediments derived from felsic source rocks, but ratios of the low-Al meta-pelites contrast obviously with those of felsic rocks and are similar to that of mafic rocks, suggesting that more mafic rocks make a contribution to their provenance (Table 2). On the La/Th versus Hf plot (Fig. 11), all data from the high-Al meta-pelites and meta-arenites show a mixing trend between felsic and recycled old sedimentary sources in different proportions, whereas the low-Al meta-pelite samples are plotted in the mixed felsic/basic field, which imply again above source characteristics of these metasediments.

Because of their geochemically similar behavior and low solubilities in water, REE have proven to provide a powerful tool for characterizing provenances when applied to sedimentary rocks (MacDaniel et al., 1994). In general, mafic volcanics range from LREE-depleted (tholeiitic) through LREE-enriched (calc-alkaline) with little Eu anomalies, while more silicic rocks are usually LREE-enriched with distinct negative Eu anomalies (Cullers et al., 1997). The Yuanjiacun metasediments are LREE-enriched ($(La/Yb)_N = 1.73–21.2$) of almost flat HREE segments ($(Gd/Yb)_N = 1.03–2.14$). These features, coupled with negative Eu anomalies for the high-Al meta-pelites and meta-arenites, denote that the original source may be felsic. However, for the low-Al meta-pelites with distinct Eu anomalies, variable mixing of felsic and mafic compositions would tend to lead to their REE patterns.

Neodymium isotopic data in combination with geochemical features can be instrumental in understanding the nature of sediment sources (McLennan et al., 1995). Fig. 12a plots ε_{Nd} ($t = 2.3$ Ga) against the Th/Sc ratio. Shown for reference is the location of the typical upper crust, intermediate island arc compositions, and MORB at 2.3 Ga. The meta-arenite and high-Al meta-pelite samples have low $\varepsilon_{Nd}(t)$ values (<0), as low as −4.3, with Th/Sc ratios close to 1. These attributes are similar to those of stable shelf shales reported by McLennan et al. (1995), reflecting that these metasediments are generally derived from the old crust and likely formed in the passive margin setting. Additionally, the T_{DM} of these metasediments ranges from 2.9 to 2.7 Ga, suggesting that they have a long crustal residence history and that the protoliths were predominantly derived from ancient crust. Moreover, the measured Th/U ratios of the metasediments are mostly greater than 3.0 and are accompanied by relatively high Th and U abundances (Appendix Table 1), precluding their derivation from the depleted mantle sources of the volcanic arcs (McLennan et al., 1993). However, the low-Al meta-pelites have consistently positive $\varepsilon_{Nd}(t)$ values, and there is a positive correlation between $\varepsilon_{Nd}(t)$ and TFe_2O_3. Considering that these samples are closely associated with the Yuanjiacun BIF and large amounts of hematite are found in thin sections (Fig. 4d), it is likely that they are mixing products of compositions of clastic (normal pelites) and chemical (BIFs) sediments. The neodymium isotopic compositions of the BIFs commonly originate from a dominantly depleted mantle source (Alexander et al., 2009). For instance, the consistently positive $\varepsilon_{Nd}(t)$ values of the Anshan BIFs in China range from 0.5 to 4.8 (Dai, 2014). Moreover, the above distinct geochemical features of the low-Al meta-pelites are more likely attributed to this certain mixing.

In addition, the U–Pb ages of detrital zircons from the meta-arenite samples can provide further information about their source rocks. The age histogram of 51 detrital zircon analyses displays some major age peaks. The major population exhibits an age range between 2.6 and 2.5 Ga with a peak of ca. 2529 Ma (Fig. 8), and minor amounts of detrital zircons are older, aged between 2.8 and 2.6 Ga. These old Archean

Table 2
Range of distinctive elemental ratios of the Yuanjiacun Formation metasediments compared to those in the average upper continental crust (Rudnick and Gao, 2003) and sediments derived from felsic and mafic rocks (Amstrong-Altrin et al., 2004).

Elemental ratio	Low-Al meta-pelites	High-Al meta-pelites	Meta-arenite	Range of sediments from felsic sources	Range of sediments from mafic sources	Upper continental crust
La/Sc	0.51–1.53	0.69–1.95[a]	3.67–5.28	2.50–16.3	0.43–0.86	2.21
Th/Sc	0.08–0.26	0.88–1.91	0.78–0.99	0.84–20.5	0.05–0.22	0.75
Eu/Eu*	0.59–1.12	0.55–0.72[a]	0.81–0.97	0.40–0.94	0.71–0.95	0.71

[a] Sample WY12-7 is excluded due to an abnormally high amount of LREE.

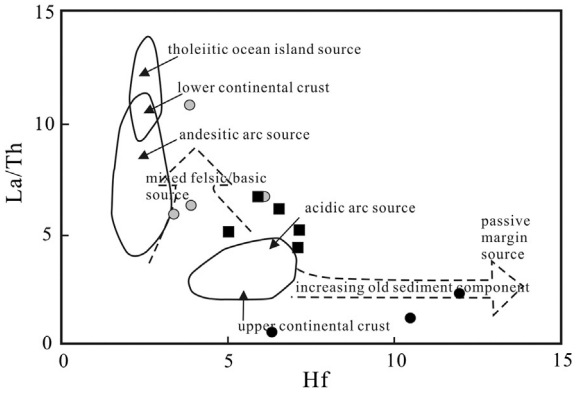

Fig. 11. Source rock discrimination diagrams for the Yuanjiacun Formation metasediments on La/Th vs. Hf (modified after Floyd and Leveridge, 1987) (same symbols as in Fig. 5). Average reference compositions are from Condie (1993).

detrital zircons must have been transported from other sources because no similarly aged lithologies or zircons have been found in the Lüliang Complex. The possible sources for these zircons are the old continental crust (likely the Ordos Block), although the Archean basement rocks in this region are rarely exposed, and the adjacent Fuping, Wutai, and Hengshan Complexes of which the majority are arc-related igneous rocks, including the Wutai volcanic rocks and granitoids and the Hengshan and Fuping TTG gneisses, were formed in the period between 2560 and 2520 Ma (Zhao et al., 2002; Wilde et al., 2004, 2005; Kröner et al., 2005a, 2005b; Zhao et al., 2007). Moreover, minor 2.85–2.60 Ga rocks and xenocrystic zircons have recently been found as remnants of an old crustal component in the Hengshan–Wutai–Fuping belt. For example, in the Fuping Complex, xenocrystic zircons from a medium-grained hornblende gneiss enclosed in the Fuping granitoid gneisses were dated by Guan et al. (2002) at 2708 ± 8 Ma. In the Hengshan Complex, a gray trondhjemitic gneiss and a gray biotite gneiss were dated by Kröner et al. (2005b) at 2712 ± 2 Ma and 2701 ± 5.5 Ma, respectively. Wilde et al. (2004) found two xenocrystic zircons with a weighted mean $^{207}Pb/^{206}Pb$ age of 2712 ± 2 Ma in the Wutai meta-andesite.

On the other hand, a subordinate younger population of detrital zircons from the meta-arenites has an age range between 2.5 and 2.3 Ga, which is consistent with the ages of the lithologic units in the Lüliang Complex. The felsic rocks within such an age range are represented by the Yunzhongshan tonalitic gneiss (2499 ± 9 Ma; Zhao et al., 2008b) and the Gaijiazhuang porphyritic granitic gneiss (2375 ± 10 Ma; Zhao et al., 2008b), which are exposed in the northeastern and central parts of the Lüliang Complex, respectively. This denotes that the population of detrital zircons in the studied sample was likely directly sourced from the Paleoproterozoic granitoid plutons in the Lüliang Complex.

5.6. Tectonic setting

Many workers have long endeavored to distinguish the tectonic conditions prevalent during the deposition of sediments on the basis of their petrography of framework grains, geochemistry, and neodymium isotopes (McLennan et al., 1990, 1993; Roser and Korsch, 1986). Considering that the low-Al pelites represent the mixing of compositions of normal pelites and typical BIFs, they are precluded from the following discussion. The high-Al pelites and arenites are thought to be deposited as multicycled sediments or under tropical conditions with low relief and sedimentation rates based on their aforementioned geochemical features. Moreover, these samples display high Th/Sc (≈1), and high Th/U (>3.8) and evolved major element compositions (e.g., high Si/Al

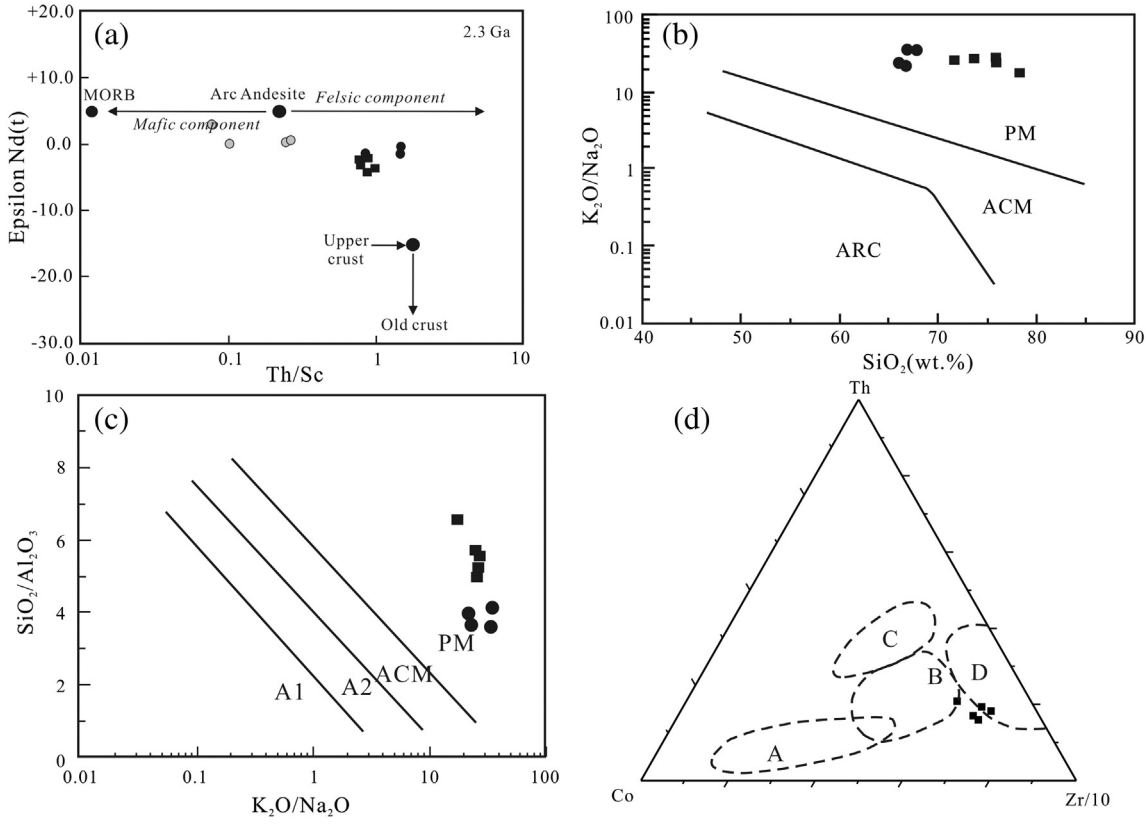

Fig. 12. (a) ε_{Nd}(2.3 Ga) vs. Th/Sc diagrams of the meta-pelite samples. End member compositions are from McLennan et al. (1993). Tectonic discrimination diagrams for the Yuanjiacun Formation metasediments including (b), (c) and (d). (b) K_2O/Na_2O versus SiO_2 and (c) SiO_2/Al_2O_3 versus K_2O/Na_2O (after Roser and Korsch, 1986). PM, passive margin; ACM, active continental margin; ARC, oceanic island-arc margin; A1, arc setting, basaltic and andesitic detritus; A2, evolved arc setting, felsic–plutonic detritus. (d) Th–Co–Zr/10 (after Bhatia and Crook, 1986). A, Oceanic island arc; B, continental island arc; C, active continental margin; D, passive margin. Symbols are the same as in Fig. 5.

and CIA (>70)) and low $\varepsilon_{Nd}(t)$ values (<0), as low as −4.3, which are most similar to those of the old Upper Continental Crust (McLennan et al., 1995). These characteristics suggest that they are likely to form in a stable cratonic setting. Detailed sedimentological study of these metasediments and the Yuanjiacun BIF (Tian et al., 1986; Wang et al., 2015) further reveals that deposition of the Yuanjiacun Formation occurred in a relatively shallow marine environment, essentially on the stable shelf.

Roser and Korsch (1986) have shown that sandstone–mudstone suits from different tectonic settings can be distinguished on the basis of the K_2O/Na_2O and SiO_2/Al_2O_3 values and SiO_2 contents. On the K_2O/Na_2O versus SiO_2 and SiO_2/Al_2O_3 versus K_2O/Na_2O plots (Fig. 12b and c), all samples of high-Al pelites and arenites from the Yuanjiacun Formation plot in the passive continental margin (PM).

Several immobile elements, such as Co, Th, and Zr, are more useful in distinguishing the tectonic environment than the major elements (Bhatia and Crook, 1986; McLennan et al., 1993). The most widespread tectonic discriminatory plots for the clastic sediments were compiled by Bhatia and Crook (1986) based on a detailed geochemical study of graywacke. For the studied meta-arenites, petrographical indications, such as the low content of poorly sorted, angular quartz grains, the presence of well-defined bedding, and the oriented mica-flakes (Fig. 4f) all point towards the meta-arenites not being an immature meta-graywacke, although geochemical data indicate that some meta-arenite samples belong to the graywacke. Therefore, these plots are not suitable for the meta-arenite samples, but can only provide some reference information. For example, the studied meta-arenite samples on the Th–Co–Zr ternary diagram (Fig. 12d, Bhatia and Crook, 1986) are plotted in and close to the passive continental margin field.

In conclusion, we suggest a passive margin setting for the depositional basin of these sediments. The absence of syn-depositional igneous rocks in the Lüliang area provides further evidence (Zhao et al., 2008b). This setting obviously contrasts with the volcanic arc setting (Liu et al., 2012) or a continental rift environment (Geng et al., 2003; Yu et al., 1997b) for the overlying meta-basalts in the Jinzhouyu Formation and meta-rhyolites in the Dujiagou Formation. The underlying Yuanjiacun and Peijiazhuang formations consist predominantly of quartzite–shale successions (Fig. 2), indicating a quiescent epicontinental marine environment. Moreover, there is a parallel unconformity between them and the overlying volcanic rocks, which is represented by the presence of a set of basal conglomerate located in the lowermost part of the Jinzhouyu Formation (Tian et al., 1986; Yu et al., 1997a). These features also argue for a distinct depositional environment for the Yuanjiacun Formation.

6. Conclusion

On the basis of the presented geochronological and geochemical analyses and Sm–Nd isotopic data of the Paleoproterozoic metasediments associated with the Yuanjiacun BIF, the following conclusions are supported:

(1) The Yuanjiacun Formation metasediments were deposited between 2350 and 2200 Ma.
(2) Source rocks of the low-Al meta-pelites have undergone severe chemical weathering, whereas those of the meta-arenites and high-Al meta-pelites had suffered moderate chemical weathering.
(3) The meta-arenites and high-Al meta-pelites are sedimentary erosion products of the less differential felsic terrain (likely the old upper continental crust), whereas the low-Al meta-pelites are regarded as mixtures of compositions of normal pelite and typical BIFs.
(4) The major sediments were most likely sourced from both the Archean igneous rocks in the Wutai area and old hidden Archean basement rocks in the Western Block, whereas minor amounts of 2.5–2.3 Ga detrital zircons were likely derived from the early Paleoproterozoic granitoid rocks in the Lüliang Complex.
(5) The high-Al meta-pelites and meta-arenites are in general geochemically mature and have suffered a greater degree of sedimentary recycling and sorting. Nevertheless, the low-Al meta-pelites bear some geochemical features typical for immature sediments, which may infer their relatively low degree of sedimentary recycling.
(6) The Yuanjiacun Formation had been originally deposited in a passive margin setting, most probably on a stable continental shelf.

Supplementary data to this article can be found online at http://dx.doi.org/10.1016/j.lithos.2014.11.015.

Acknowledgments

This research was financially supported by the Major State Basic Research Programme of the People's Republic of China (No. 2012CB416601), the National Natural Science Foundation of China (No. 41372100) and the Knowledge Innovation Programme of the Chinese Academy of Sciences (No. KZCX2-YW-Q04-07). Much thanks to Peng Xiang, Mengtian Zheng and Zhiquan Li, for their help in LA–ICP-MS analyses. We thank Xindi Jin, Wenjun Li and Bingyu Gao for their laboratory assistance. We also thank Dr. Sun-Lin Chung and two anonymous reviewers for their constructive comments.

References

Alexander, B.W., Bau, M., Andersson, P., 2009. Neodymium isotopes in Archean seawater and implications for the marine Nd cycle in Earth's early oceans. Earth and Planetary Science Letters 283, 144–155.
Amstrong-Altrin, J.S., Lee, Y.I., Verma, S.P., Ramasamy, S., 2004. Geochemistry of sandstones from the Upper Miocene Kudankulam Formation, southern India: implications for provenance, weathering, and tectonic setting. Journal of Sedimentary Research 74, 285–297.
Asiedu, D.K., Dampare, S.B., Asmoah Sakyi, P., Banoeng-Yakubo, B., Osae, S., Nyarko, B.J.B., Manu, J., 2004. Geochemistry of Paleoproterozoic metasedimentary rocks from the Birim diamontiferous field, southern Ghana: implications for provenance and crustal evolution at the Archean–Proterozoic boundary. Geochemical Journal 38, 215–228.
Barovich, K.M., Patchett, P.J., 1992. Behaviour of isotopic systematics during deformation and metamorphism: a Hf, Nd, and Sr isotopic study of mylonitized granite. Contributions to Mineralogy and Petrology 109, 386–393.
Bhatia, M.R., 1985. Rare earth element geochemistry of Australian Paleozoic graywackes and mud rocks: provenance and tectonic control. Sedimentary Geology 45, 97–113.
Bhatia, M.R., Crook, K.A.W., 1986. Trace element characteristics of graywackes and tectonic setting discrimination of sedimentary basins. Contributions to Mineralogy and Petrology 92, 181–193.
Bock, B., McLennan, S.M., Hanson, G.N., 1998. Geochemistry and provenance of the Middle Ordovician Austin Glen Member (Normanskill Formation) and the Taconian Orogeny in New England. Sedimentology 45, 635–655.
Condie, K.C., 1993. Chemical composition and evolution of the upper continental crust: contrasting results from surface samples and shales. Chemical Geology 104, 1–37.
Condie, K.C., Noll, P.D., Conway, C.M., 1992. Geochemical and detrital mode evidence for two sources of Early Proterozoic metasedimentary rocks from the Tonto Basin Supergroup, central Arizona. Sedimentary Geology 77, 51–76.
Cox, R., Lowe, D.R., Cullers, R.L., 1995. The influence of sediment recycling and basement composition on evolution of mudrock chemistry in the southwestern United States. Geochimica et Cosmochimica Acta 59, 2919–2940.
Cullers, R.L., 1988. Mineralogical and chemical changes of soil and stream sediments formed by intense weathering of the Danberg granite, Georgia, USA. Chemical Geology 113, 327–343.
Cullers, R.L., 1994a. The chemical signature of source rocks in size fractions of Holocene stream sediment derived from metamorphic rocks in the Wet Mountains region, USA. Chemical Geology 113, 327–343.
Cullers, R.L., 1994b. The controls on the major and trace element variation of shale, siltstones, and sandstones of Pennsylvanian–Permian age from uplifted continental blocks in Colorado to platform sediment in Kansas, USA. Geochimica et Cosmochimica Acta 58, 4955–4972.
Cullers, R.L., Bock, B., Guidotti, C., 1997. Elemental distribution and neodymium isotopic compositions of Silurian metasediments, western Maine, USA: redistribution of the rare earth elements. Geochimica et Cosmochimica Acta 61, 1847–1861.
Dai, Y.P., 2014. The Archean two-stage BIF deposition and genesis of high-grade iron ores in the Anshan–Benxi area. Doctoral Dissertation University of Chinese Academy of Sciences, p. 162.
El-Bialy, M.Z., 2013. Geochemistry of the Neoproterozoic metasediments of Malhaq and Um Zariq formations, Kid metamorphic complex, Sinai, Egypt: implications for source-area weathering, provenance, recycling, and depositional tectonic setting. Lithos 175–176, 68–85.

Fedo, C.M., Nesbitt, H.M., Young, G.M., 1995. Unraveling the effects of potassium metasomatism in sedimentary rocks and paleosols, with implications for paleoweathering conditions and provenance. Geology 23, 921–924.
Feng, R., Kerrich, R., 1990. Geochemistry of fine-grained clastic sediments in the Archean Abitibi greenstones belt, Canada: implications for provenance and tectonic setting. Geochimica et Cosmochimica Acta 54, 1061–1081.
Floyd, P.A., Leveridge, B.E., 1987. Tectonic environment of the Devonian Gramscatho basin, south Cornwall: framework mode and geochemical evidence from turbiditic sandstones. Journal of the Geological Society of London 144, 531–542.
Floyd, P.A., Shail, R., Leveridge, B.E., Franke, W., 1991. Geochemistry and provenance of Rhenohercynian synorogenic sandstones: implications for tectonic environment discrimination. In: Morton, A.C., Todd, S.P., Haughton, P.D.W. (Eds.), Developments in Sedimentary Provenance Studies 7. Geological Society Special Publication, pp. 173–188.
Fralick, P.W., Kronberg, B.I., 1997. Geochemical discrimination of clastic sedimentary rock sources. Sedimentary Geology 113, 111–124.
Garcia, D., Fonteilles, M., Moutte, J., 1994. Sedimentary fractionations between Al, Ti, and Zr and the genesis of strongly peraluminous granites. Journal of Geology 102, 411–422.
Geng, Y.S., Wan, Y.S., Shen, Q.H., Li, H.M., Zhang, R.X., 2000. Chronological framework of the Early Precambrian important events in the Lüliang Area, Shanxi Province. Acta Petrologica Sinica 74, 216–223.
Geng, Y.S., Wan, Y.S., Yang, C.H., 2003. The Palaeoproterozoic rift-type volcanism in Lüliangshan area, Shanxi Province, and its geological significance. Acta Geoscientia Sinica 24, 97–104.
Geng, Y.S., Yang, C.H., Song, B., Wan, Y.S., 2004. Post-orogenic granites with an age of 1800 Ma in Lüliang area, North China Craton: constraints from isotopic geochronology and geochemistry. Geological Journal of China Universities 10, 477–487.
Geng, Y.S., Wan, Y.S., Yang, C.H., 2008. The Set of Main Geological Events in the Paleoproterozoic Lüliang Area, Shanxi Province. Geological Publishing House, Beijing, pp. 515–533.
Gromet, L.P., Dymek, R.E., Haskin, L.A., Korotev, R.L., 1984. The North American shale composite: its composition, major and trace element characteristics. Geochimica et Cosmochimica Acta 48, 2469–2482.
Guan, H., Sun, M., Wilde, S.A., Zhou, X.H., Zhai, M.G., 2002. SHRIMP U–Pb zircon geochronology of the Fuping Complex: implications for formation and assembly of the North China Craton. Precambrian Research 113, 1–18.
Guo, J.H., O'Brien, P.J., Zhai, M.G., 2002. High-pressure granulites in the Sangan area, North China Craton: metamorphic evolution, P–T paths and geotectonic significance. Journal of Metamorphic Geology 20, 741–756.
Guo, J.H., Sun, M., Zhai, M.G., 2005. Sm–Nd and SHRIMP U–Pb zircon geochronology of high-pressure granulites in the Sanggan area, North China Craton: timing of Paleoproterozoic continental collision. Journal of Asian Earth Sciences 24, 629–642.
Harnois, L., 1988. The CIW index: a new chemical index of weathering. Sedimentary Geology 55, 319–322.
Hayashi, K., Hiroyuki, F., Heinrich, H.D., Ohmoto, H., 1997. Geochemistry of 1.9 Ga sedimentary rocks from northeastern Labrador, Canada. Geochimica et Cosmochimica Acta 61, 4115–4137.
Herron, M.M., 1988. Geochemical classification of terrigenous sands and shales from core or log data. Journal of Sedimentary Petrology 58, 820–829.
Jahn, B.M., Condie, K.C., 1995. Evolution of the Kaapvaal Craton as viewed from geochemical and Sm–Nd isotopic analyses of intracratonic pelites. Geochimica et Cosmochimica Acta 59, 2239–2258.
Kröner, A., Wilde, S.A., Li, J.H., Wang, K.Y., 2005a. Age and evolution of a late Archaean to early Palaeozoic upper to lower crustal section in the Wutaishan/Hengshan/Fuping terrain of northern China. Journal of Asian Earth Sciences 24, 577–595.
Kröner, A., Wilde, S.A., O'Brien, P.J., Li, J.H., Passchier, C.W., Walte, N.P., Liu, D.Y., 2005b. Field relationships, geochemistry, zircon ages and evolution of a late Archean to Paleoproterozoic lower crustal section in the Hengshan Terrain of Northern China. Acta Geologica Sinica (English Edition) 79, 605–629.
Kröner, A., Wilde, S.A., Zhao, G.C., O'Brien, P.J., Sun, M., Liu, D.Y., Wan, Y.S., Liu, S.W., Guo, J.H., 2006. Zircon geochronology of mafic dykes in the Hengshan Complex of northern China: evidence for late Palaeoproterozoic rifting and subsequent high-pressure event in the North China Craton. Precambrian Research 146, 45–67.
Liu, J.Z., Zhang, F.Q., Ouyang, Z.Y., Li, C.L., Zou, Y.L., Xu, L., 2001. Geochemistry and chronology of the Jiehekou Group metamorphic basic volcanic rocks in the Lüliang Mountain area, Shanxi, China. Science in China Series D-Earth Science 31, 111–118.
Liu, S.W., Zhao, G.C., Wilde, S.A., Shu, G.M., Sun, M., Li, Q.G., Tian, W., Zhang, J., 2006. Th–U–Pb monazite geochronology of the Lüliang and Wutai Complexes: constraints on the tectonothermal evolution of the Trans-North China Orogen. Precambrian Research 148, 205–224.
Liu, S.W., Li, Q.G., Liu, C.H., Lü, Y.J., Zhang, F., 2009. Guandishan granitoids of the Paleoproterozoic Luliang Metamorphic Complex in the Trans-North China Orogen: SHRIMP zircon ages, petrogenesis and tectonic implications. Acta Geologica Sinica 83, 580–602 (English edition).
Liu, S.W., Li, Q.G., Zhang, L.F., Yang, P.T., Liu, C.H., Lü, Y.J., Wu, F.H., 2010. Geology, geochemistry of metamorphic volcanic rock suite in Precambrian Yejishan Group, Lüliang mountains and its tectonic implications. Acta Petrologica Sinica 25, 547–560.
Liu, C.H., Zhao, G.C., Sun, M., Wu, F.Y., Yang, J.H., Yin, C.Q., Leung, W.H., 2011. U–Pb and Hf isotopic study of detrital zircons from the Yejishan Group of the Lüliang Complex: constraints on the timing of collision between the Eastern and Western Blocks, North China Craton. Sedimentary Geology 236, 129–140.
Liu, S.W., Zhang, J., Li, Q.G., Zhang, L.F., Wang, W., Yang, P.T., 2012. Geochemistry and U–Pb zircon ages of metamorphic volcanic rocks of the Paleoproterozoic Lüliang Complex and constraints on the evolution of the Trans-North China Orogen, North China Craton. Precambrian Research 222, 173–190.
Liu, C.H., Liu, F.L., Zhao, G.C., 2013. Provenance and tectonic setting of the Jiehekou Group in the Lüliang Complex: constraints from zircon U–Pb age and Hf isotopic studies. Acta Petrologica Sinica 29, 517–532.
MacDaniel, D.K., Hemming, S.R., McLennan, S.M., Hanson, G.N., 1994. Resetting of neodymium isotopes and redistribution of REEs during sedimentary processes: the Early Proterozoic Chelmsford Formation, Sudbury Basin, Ontario, Canada. Geochimica et Cosmochimica Acta 58, 931–941.
Mader, D., Neubauer, F., 2004. Provenance of Palaeozoic sandstones from the Carnic Alps (Austria): petrographic and geochemical indicators. International Journal of Earth Sciences 93, 262–281.
McLennan, S.M., 1989. Rare earth elements in sedimentary rocks: influence of provenance and sedimentary processes. Mineralogical Society of America Reviews in Mineralogy 21, 169–200.
McLennan, S.M., Taylor, S.R., McCulloch, M.T., Maynard, J.B., 1990. Geochemical and Nd–Sr isotopic composition of deep-sea turbidites: crustal evolution and plate tectonic associations. Geochimica et Cosmochimica Acta 54, 2015–2050.
McLennan, S.M., Hemming, S., McDaniel, D.K., Hanson, G.N., 1993. Geochemical approaches to sedimentation, provenance and tectonics. In: Johnsson, M.J., Basu, A. (Eds.), Processes Controlling the Composition of Clastic Sediments. Geological Society of America Special Paper 284, pp. 21–40.
McLennan, S.M., Hemming, S., Taylor, S.R., Eriksson, K.A., 1995. Early Proterozoic crustal evolution: geochemical and Nd–Pb isotopic evidence from metasedimentary rocks, southwestern North America. Geochimica et Cosmochimica Acta 59, 1153–1177.
Nesbitt, H.W., Young, G.M., 1982. Early Proterozoic climates and plate motions inferred from major element chemistry of lutites. Nature 299, 715–717.
Nesbitt, H.W., Young, G.M., 1984. Prediction of some weathering trends of plutonic and volcanic rocks based on thermodynamic and kinetic considerations. Geochimica et Cosmochimica Acta 48, 1423–1534.
Nesbitt, H.W., Young, G.M., 1989. Formation and diagenesis of weathering profiles. Journal of Geology 97, 129–147.
Nesbitt, H.W., Markovics, G., Price, R.C., 1980. Chemical processes affecting alkalis and alkaline earth during continental weathering. Geochimica et Cosmochimica Acta 44, 1659–1666.
Pearce, J.A., 1996. A user's guide to basalt discrimination diagrams. In: Wyman, D.A. (Ed.), Trace Element Geochemistry of Volcanic Rocks: Application for Massive Sulphide Exploration. Mineralogical Association of Canada Short Course 12, pp. 79–113.
Roddaz, M., Viers, J., Brusset, S., Baby, P., Boucayrand, C., Hérail, G., 2006. Controls on weathering and provenance in the Amazonian foreland basin: insights from major and trace element geochemistry of Neogene Amazonian sediments. Chemical Geology 226, 31–65.
Rollinson, H.R., 1993. Using Geochemical Data: Evolution, Presentation, Interpretation. Longman, Essex, England, pp. 1–352.
Roser, B.P., Korsch, R.J., 1986. Determination of tectonic setting of sandstone–mudstone suites using SiO_2 content and K_2O/Na_2O ratio. Journal of Geology 94, 635–650.
Roser, B.P., Korsch, R.J., 1988. Provenance signatures of sandstone–mudstone suite determined using discrimination function analysis of major-element data. Chemical Geology 67, 119–139.
Roser, B.P., Cooper, R.A., Nathan, S., Tulloch, A.J., 1996. Reconnaissance sandstone geochemistry, provenance, and tectonic setting of the lower Paleozoic terranes of the West Coast and Nelson, New Zealand. New Zealand Journal of Geology and Geophysics 39, 1–16.
Rudnick, R.L., Gao, S., 2003. The composition of the continental crust. In: Rudnick, R.L. (Ed.), The Crust. Elsevier-Pergamon, Oxford, pp. 1–64.
Shen, B.F., Zhai, A.M., Yang, C.L., 2010. Paleoproterozoic—an important metallogenic epoch in China. Geological Survey and Research 33, 241–256.
Sun, S.S., McDonough, W.F., 1989. Chemical and isotopic systematics of oceanic basalts: implications for mantle composition and processes. In: Saunders, A.D., Norry, M.J. (Eds.), Magmatism in the Ocean Basins. Special Publications 42. Geological Society, London, pp. 313–345.
Taylor, S.R., McLennan, S.M., 1985. The Continental Crust: Its Composition and Evolution. Blackwell Scientific Publishers, Oxford.
Tian, Y.Q., Yuan, G.P., Lu, J.R., Jing, Y., Yu, J.H., Li, M.M., 1986. Research on formation conditions and tectonic characteristics of Precambrian Yuanjiacun metamorphic–sedimentary iron deposits in Lan County, Shanxi province. Geology and Mineral Resources Bureau Press, Shanxi.
Trap, P., Faure, M., Lin, W., Monié, P., 2007. Late Paleoproterozoic (1900–1800 Ma) nappe stacking and polyphase deformation in the Hengshan–Wutaishan area: implications for the understanding of the Trans-North-China Belt, North China Craton. Precambrian Research 156, 85–106.
Wan, Y.S., Geng, Y.S., Shen, Q.H., Zhang, R.X., 2000. Khondalite series—geochronology and geochemistry of the Jiehekou Group in Lüliang area, Shanxi Province. Acta Petrologica Sinica 16, 49–58.
Wan, Y.S., Song, B., Liu, D.Y., Wilde, S.A., Wu, J.S., Shi, Y.R., Yin, X.Y., Zhou, H.Y., 2006a. SHRIMP U–Pb zircon geochronology of Palaeoproterozoic metasedimentary rocks in the North China Craton: evidence for a major Late Palaeoproterozoic tectonothermal event. Precambrian Research 149, 249–271.
Wan, Y.S., Wilde, S.A., Liu, D.Y., Yang, C.X., Song, B., Yin, X.Y., 2006b. Further evidence for 1.85 Ga metamorphism in the central Zone of the north China Craton: SHRIMP U–Pb dating of zircons from metamorphic rocks in the Lushan area, Henan Province. Gondwana Research 9, 189–197.
Wang, W., Chen, F.K., Hu, R., Chu, Y., Yang, Y.Z., 2012. Provenance and tectonic setting of Neoproterozoic sedimentary sequences in the South China Block: evidence from

detrital zircon ages and Hf–Nd isotopes. International Journal of Earth Science 101, 1723–1744.
Wang, C.L., Zhang, L.C., Lan, C.Y., Li, H.Z., Huang, H., 2015. Analysis of sedimentary facies and depositional environment of the Yuanjiacun banded iron formation in the Lüliang area, Shanxi Province. Acta Petrologica Sinica accepted.
Wilde, S.A., Zhao, G.C., 2005. Archean to Paleoproterozoic evolution of the North China Craton. Journal of Asian Earth Sciences 24, 519–522.
Wilde, S.A., Cawood, P.A., Wang, K.Y., Nemchin, A., 2005. Granitoid evolution in the Late Archaean Wutai Complex, North China Craton. Journal of Asian Earth Sciences 24, 597–613.
Wilde, S.A., Cawood, P.A., Wang, K.Y., Nemchin, A., Zhao, G.C., 2004. Determining Precambrian crustal evolution in China: a case-study from Wutaishan, Shanxi Province, demonstrating the application of precise SHRIMP U–Pb geochronology. In: Malpas, J., Fletcher, C.J.N., Ali, J.R., Aichison, J.C. (Eds.), Aspects of the Tectonic Evolution of China: Geological Society of London. Special Publication 226, pp. 5–26.
Xia, X.P., Sun, M., Zhao, G.C., Wu, F.Y., Xie, L.W., 2009. U–Pb and Hf isotopic study of detrital zircons from the Lüliang khondalite, North China Craton, and their tectonic implications. Geological Magazine 146, 701–716.
Yao, P.H., 1993. Records of Chinas Iron Ore Deposits. (in Chinese) Metallurgical Industry Press, Beijing, pp. 1–662.
Yu, J.H., Wang, D.Z., Wang, C.Y., 1997a. Ages of the Lüliang group and its main metamorphism in the Lüliang mountains, Shanxi—evidence from single-grain zircon U–Pb ages. Geological Review 43, 403–408.
Yu, J.H., Wang, D.Z., Wang, C.Y., 1997b. Geochemical characteristics and petrogenesis of the Early Proterozoic bimodal volcanic rocks from Lüliang Group, Shanxi Province. Acta Petrologica Sinica 13, 59–70.
Zhai, M.G., Guo, J.H., Yang, Y.H., 1992. Discovery and preliminary study of the Archean high-pressure granulites in the North China. Science in China Series D-Earth Sciences 12B, 1325–1330.
Zhai, M.G., Guo, J.H., Li, H.H., Yang, Y.H., Li, Y.G., 1995. Discovery of retrograded eclogites in the Archaean North China Craton. Chinese Science Bulletin 40, 1590–1594.
Zhang, J., Zhao, G.C., Li, S.Z., Sun, M., Liu, S.W., Wilde, S.A., Kröner, A., Yin, C.Q., 2007. Deformation history of the Hengshan Complex: implications for the tectonic evolution of the Trans-North China Orogen. Journal of Structural Geology 29, 933–949.
Zhao, G.C., Zhai, M.G., 2013. Lithotectonic elements of Precambrian basement in the North China Craton: review and tectonic implications. Gondwana Research 23, 1207–1240.
Zhao, G.C., Wilde, S.A., Cawood, P.A., Lu, L.Z., 1998. Thermal evolution of the Archaean basement rocks from the eastern part of the North China Craton and its bearing on tectonic setting. International Geology Review 40, 706–721.
Zhao, G.C., Wilde, S.A., Cawood, P.A., Sun, M., 2001. Archean blocks and their boundaries in the North China Craton: lithological, geochemical, structural and P–T path constraints and tectonic evolution. Precambrian Research 107, 45–73.
Zhao, G.C., Wilde, S.A., Cawood, P.A., Sun, M., 2002. SHRIMP U–Pb zircon ages of the Fuping Complex: implications for late Archean to Paleoproterozoic accretion and assembly of the North China Craton. American Journal of Science 302, 191–226.
Zhao, G.C., Sun, M., Wilde, S.A., Li, S.Z., 2005. Late Archean to Paleoproterozoic evolution of the North China Craton: key issues revisited. Precambrian Research 136, 177–202.
Zhao, G.C., Kröner, A., Wilde, S.A., Sun, M., Li, S.Z., Li, X.P., Zhang, J., Xia, X.P., He, Y.H., 2007. Lithotectonic elements and geological events in the Hengshan–Wutai–Fuping belt: a synthesis and implications for the evolution of the Trans-North China Orogen. Geological Magazine 144, 753–775.
Zhao, G.C., Wilde, S.A., Sun, M., Guo, J.H., Kröner, A., Li, S.Z., Li, X.P., Wu, C.M., 2008a. SHRIMP U–Pb zircon geochronology of the Huaian Complex: constraints on Late Archean to Paleoproterozoic crustal accretion and collision of the Trans-North China Orogen. American Journal of Science 308, 270–303.
Zhao, G.C., Wilde, S.A., Sun, M., Li, S.Z., Li, X.P., Zhang, J., 2008b. SHRIMP U–Pb zircon ages of granitoid rocks in the Lüliang Complex: implications for the accretion and evolution of the Trans-North China Orogen. Precambrian Research 160, 213–226.